

Discovery and Synthesis of a Phosphoramidate Prodrug of a Pyrrolo[2,1-*f*][triazin-4-amino] Adenine C-Nucleoside (GS-5734) for the Treatment of Ebola and Emerging Viruses

Dustin Siegel,<sup>†</sup> Hon C. Hui,<sup>†</sup> Edward Doerffler,<sup>†</sup> Michael O. Clarke,<sup>†</sup> Kwon Chun,<sup>†</sup> Lijun Zhang,<sup>†</sup> Sean Neville,<sup>†</sup> Ernest Carra,<sup>†</sup> Willard Lew,<sup>†</sup> Bruce Ross,<sup>†</sup> Queenie Wang,<sup>†</sup> Lydia Wolfe,<sup>†</sup> Robert Jordan,<sup>†</sup> Veronica Soloveva,<sup>‡</sup> John Knox,<sup>†</sup> Jason Perry,<sup>†</sup> Michel Perron,<sup>†</sup> Kirsten M. Stray,<sup>†</sup> Ona Barauskas,<sup>†</sup> Joy Y. Feng,<sup>†</sup> Yili Xu,<sup>†</sup> Gary Lee,<sup>†</sup> Arnold L. Rheingold,<sup>§</sup> Adrian S. Ray,<sup>†</sup> Roy Bannister,<sup>†</sup> Robert Strickley,<sup>†</sup> Swami Swaminathan,<sup>†</sup> William A. Lee,<sup>†</sup> Sina Bavari,<sup>‡</sup> Tomas Cihlar,<sup>†</sup> Michael K. Lo,<sup>||</sup> Travis K. Warren,<sup>‡</sup> and Richard L. Mackman<sup>\*,†,||</sup>

<sup>†</sup>Gilead Sciences, Inc., Foster City, California 94404, United States

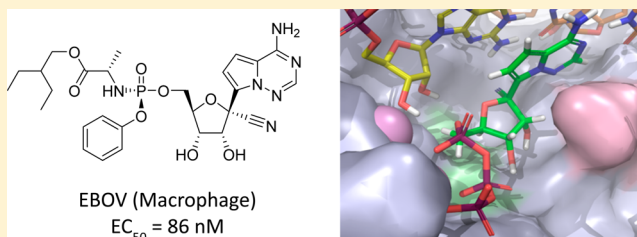
<sup>‡</sup>United States Army Medical Research Institute of Infectious Diseases (USAMRIID), Frederick, Maryland 21702, United States

<sup>§</sup>University of California—San Diego, San Diego, California 92093, United States

<sup>||</sup>Centers for Disease Control and Prevention, Atlanta, Georgia 30333, United States

**S** Supporting Information

**ABSTRACT:** The recent Ebola virus (EBOV) outbreak in West Africa was the largest recorded in history with over 28,000 cases, resulting in >11,000 deaths including >500 healthcare workers. A focused screening and lead optimization effort identified **4b** (GS-5734) with anti-EBOV EC<sub>50</sub> = 86 nM in macrophages as the clinical candidate. Structure activity relationships established that the 1'-CN group and C-linked nucleobase were critical for optimal anti-EBOV potency and selectivity against host polymerases. A robust diastereoselective synthesis provided sufficient quantities of **4b** to enable preclinical efficacy in a non-human-primate EBOV challenge model. Once-daily 10 mg/kg iv treatment on days 3–14 postinfection had a significant effect on viremia and mortality, resulting in 100% survival of infected treated animals [*Nature* **2016**, *531*, 381–385]. A phase 2 study (PREVAIL IV) is currently enrolling and will evaluate the effect of **4b** on viral shedding from sanctuary sites in EBOV survivors.

**■ INTRODUCTION**

Ebola virus disease (EVD) was first documented 40 years ago during an outbreak of infectious hemorrhagic fever in Northern Zaire (current Democratic Republic of Congo). More than 20 intermittent outbreaks have occurred since then, but the most recent outbreak in West Africa spanning 2013–2016 has been the largest recorded in history and presented an international public health emergency.<sup>1</sup> Over 28,000 cases were confirmed in Guinea, Liberia, and Sierra Leone resulting in >11,000 deaths including >500 healthcare workers, which severely strained the local medical infrastructure.<sup>2</sup> In survivors, the Ebola virus (EBOV) can persist in bodily fluids for months after the onset of acute infection potentially leading to EVD-related sequelae and viral recrudescence.<sup>3</sup> While rare, secondary transmission has been documented to occur through sexual intercourse implicating persistent virus in genital secretions.<sup>4</sup> Despite the end of the current outbreak, the potential for equally devastating future outbreaks together with the persistent virus observed in survivors makes the development of a safe,

effective, and readily available treatment option for EVD a high priority.

EBOV, a member of the *Filoviridae* family, is a single-stranded, negative-sense, nonsegmented RNA virus that is the causative agent of EVD. Other *Filoviridae* family members include Marburg, Sudan, and Bundibugyo viruses, which have all been responsible for outbreaks associated with high mortality rates in sub-Saharan Africa.<sup>5,6</sup> Over the course of the recent West African EVD outbreak, several direct acting anti-Ebola agents including monoclonal antibodies (ZMapp),<sup>7</sup> interfering-RNAs,<sup>8–10</sup> and small molecule nucleoside(tide) antivirals such as favipiravir (**1**),<sup>11–13</sup> and brincidofovir (**2**)<sup>14</sup> have been evaluated in early clinical trials (Figure 1). More recently another nucleoside analogue, galidesivir (**3**, BCX4430<sup>15</sup>), has entered clinical development. These developments are encouraging, but to date, none of these potential therapeutics have established robust clinical efficacy for the

Received: October 27, 2016

Published: January 26, 2017

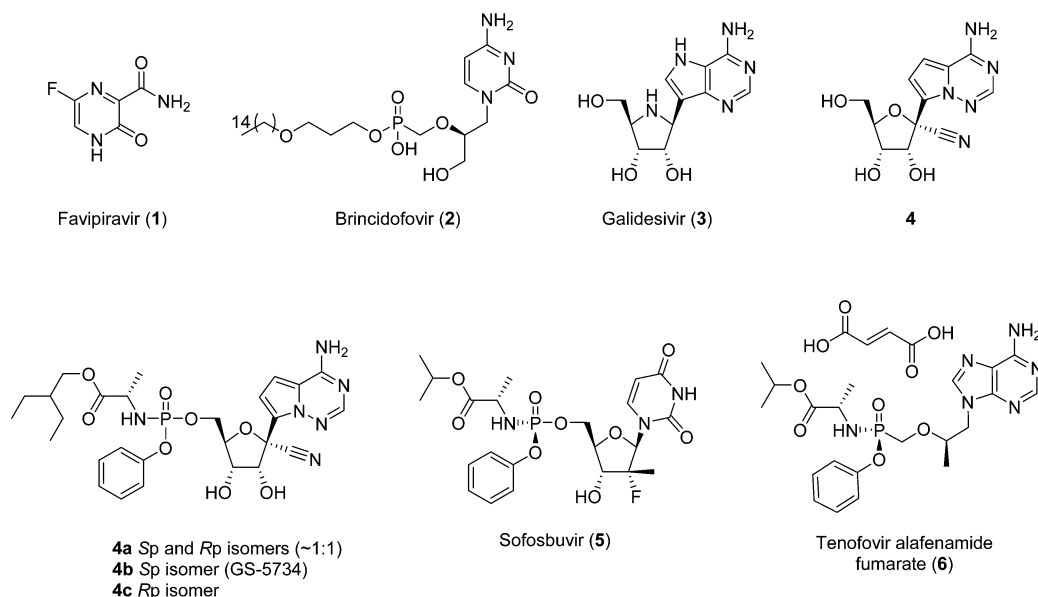


**Figure 1.** Structures of antiviral nucleosides and nucleoside phosphonates.

treatment of acute infection or the viral persistence and sequelae. Several vaccines have shown strong promise for preventing EBOV infection, but the breadth and durability of protection they can afford has yet to be established.<sup>16</sup>

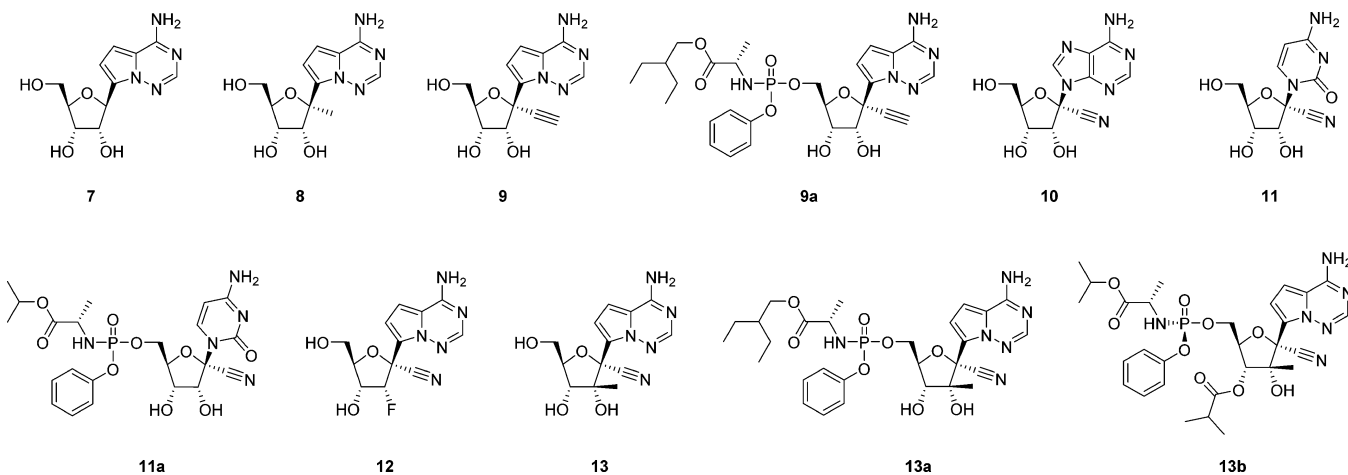
Prior to the Ebola outbreak, we had embarked on a strategic initiative aimed at evaluating the potential of nucleoside analogues for the treatment of selected emerging viruses. A library of ~1000 diverse nucleoside and nucleoside phosphonate analogues was harnessed from over 2 decades of research across multiple antiviral programs. In collaboration with the Center for Disease Control and Prevention (CDC) and the United States Army Medical Research Institute of Infectious Diseases (USAMRIID), selected compounds from the library were screened against EBOV, leading to the identification of parent **4** and a potent monophosphate prodrug mixture **4a** that contained the single Sp isomer **4b** (GS-5734<sup>17</sup>) that was selected for development. This report describes in detail the structure activity relationships (SAR) of the parent nucleoside, prodrug optimization and selection, and synthesis optimization of the development candidate **4b**. Candidate compound **4b** is currently in phase 2 trials to assess the effect on the chronic shedding of virus in EVD survivors following promising efficacy data established in a non-human-primate (NHP) EVD challenge model. These data have been recently reported<sup>17</sup> and will be summarized along with the early clinical experience with **4b**.

## RESULTS AND DISCUSSION

The assembly of the ~1000 compound nucleos(t)ide screening library was heavily focused toward ribose analogues that could target RNA viruses since this would encompass many emerging viral infections ranging from respiratory pathogens belonging to the *Coronaviridae* family such as severe acute respiratory syndrome (SARS) and Middle East respiratory syndrome (MERS), to mosquito-borne viruses of the *Flaviviridae* family such as Dengue and Zika. The majority of the library compounds were nucleosides that contained a cyclic modified ribose or “ribose-like” core. These nucleosides were also predominantly *N*-nucleosides. Less than 10% of the library comprised nucleoside phosphonates or acyclic analogues due to

the limited success, to date, in identifying potent RNA virus inhibitors with these types of analogs. A second key factor in the library assembly was that approximately 50% of the library included monophosphate and ester prodrugs to capture analogs that may be missed in cellular screens due to either poor permeability or inefficient metabolism in the respective cell types that the different antiviral assays utilize. Nucleoside analogs require activation by intracellular nucleoside/tide kinases to generate their respective nucleoside triphosphate (NTP) metabolites in order to then compete with endogenous natural nucleotide pools for incorporation into the replicating viral RNA.<sup>17</sup> The first phosphorylation step to generate the nucleoside monophosphate is often rate limiting, and therefore the application of monophosphate prodrugs, especially phosphoramidates (ProTides), has been extensively explored in nucleoside analogs to bypass this initial phosphorylation step.<sup>18</sup> A notable example includes the phosphoramidate prodrug Sofosbuvir (**5**) for the treatment of HCV (Figure 1).<sup>19</sup> Nucleoside phosphonate analogs are bioisosteres of the monophosphates but also require prodrugs to enable masking of the charged phosphonate acid thereby allowing more efficient entry into cells. A recent example of an approved drug in this class is the phosphoramidate prodrug tenofovir alafenamide (**6**) for the treatment of HIV.<sup>20</sup> In both examples the amidate prodrugs effectively deliver high levels of triphosphate (diphosphosphonate in the case of nucleoside phosphonates) inside the target cells and demonstrate significant improvements in potency compared to their respective parent nucleos(t)ides when screened in antiviral assays.<sup>20,21</sup>

In the original library screening toward a panel of RNA viruses across different viral families, promising leads were identified. Subsequent to the EVD outbreak, some of these analogs were selected for EBOV testing in collaboration with the CDC and USAMRIID in a BSL-4 facility. From this screen nucleoside **4**,<sup>22</sup> a 1'-CN modified adenosine C-nucleoside emerged with sub-micromolar activity toward EBOV in human microvascular endothelial cells (HMVEC-TERT) cells (entry 2, Table 1). In addition, its phosphoramidate prodrug mixture **4a**<sup>23</sup> (entry 3, Table 1) containing ~1:1 ratio of Sp **4b** and Rp

Table 1. SAR of Nucleoside Parents and Selected Prodrugs<sup>a</sup>

entry	compd	EBOV EC <sub>50</sub> HeLa cells (μM)	EBOV EC <sub>50</sub> HMVEC cells <sup>b</sup> (μM)	RSV EC <sub>50</sub> HEP-2 cells (μM)	HCV 1b EC <sub>50</sub> Huh-7 cells (μM)	CC <sub>50</sub> HEP-2 cells (μM)	CC <sub>50</sub> Huh-7 cells (μM)	CC <sub>50</sub> MT4 cells (μM)
1	7							<0.01
2	4	>20	0.78	0.53	4.1	>100	>88	>57
3	4a	0.17	0.12	0.027	0.023 <sup>d</sup>	9.2	17 <sup>d</sup>	2.0
4	4b	0.10	0.053	0.015	0.057	6.1	36	1.7
5	8		>10	5.5	38	93	62	4.5
6	9			>200	>88	>200	>88	120
7	9a		3.9	1.1	6.9	>100	>44	>32
8	10		56	>100	>44	>100	>88	>53
9	11	>50	>10	7.3	12	>100	>44	>57
10	11a	>20		63	2.5	>100	>44	53
11	12			>100 <sup>c</sup>	>44		>44	32 <sup>c</sup>
12	13	50	>10	>100	>44	>100	>44	>57
13	13a	27	13 <sup>d</sup>	>50	0.37	>50	>44	1.4
14	13b	>20	40	>20	0.31	95	51	7.8

<sup>a</sup>Data reported are at least  $n \geq 2$  in 384 well assay format unless otherwise noted. <sup>b</sup>HMVEC cells = TERT-immortalized human foreskin microvascular endothelial cells (ATCC-4025) cells. <sup>c</sup>96 well assay format. <sup>d</sup> $n = 1$  data only.

4c diastereoisomers (Figure 1) was found to be very potent toward EBOV in both HeLa and HMVEC cells. Encouraged by these data, the anti-EBOV activity for a range of nucleoside analogs and their prodrugs was evaluated and the results are reported in Table 1, along with activity toward respiratory syncytial virus (RSV), from the *Pneumoviridae* family, and HCV, from the *Flaviviridae* family.

The presence of the 1'-CN modification in 4 was found to be critical in providing selectivity toward viral polymerases and avoiding the significant toxicity ( $CC_{50} < 0.01$ – $0.15 \mu\text{M}$ ) associated with the unmodified C-nucleoside 7 (entry 1, Table 1).<sup>24</sup> The MT4 cell line was also used as a sensitive cell line to evaluate cytostatic effects of nucleoside analogs and confirmed the poor selectivity of 7 observed in both the HEP-2 and Huh-7 cell lines. The prodrug mixture 4a, in addition to potent anti-EBOV activity, demonstrated significant activity toward RSV and HCV, with potencies similar to or better than that for EBOV ( $EC_{50} < 120 \text{ nM}$ ). The broad and potent antiviral activity across all three viruses for 4a was further supported by the potent activity of the single Sp isomer 4b toward the same viruses and also other emerging RNA viruses such as MERS and Junin viruses, and to a lesser extent Lassa.<sup>17</sup> The antiviral selectivity of 4b toward EBOV was 17–32-fold compared to the MT4 cell line  $CC_{50}$ , and higher in the other cell types reported in Table 1. Given the anticipated short treatment duration for EVD, this window of in vitro selectivity was

considered sufficient for continued interest in 4b. The 1'-methyl analogue 8 (entry 5)<sup>22</sup> was less active toward EBOV and also displayed a higher degree of toxicity compared to the 1'-CN analogue 4 illustrating how small changes in the polarity and size of the 1' substituent can impact the overall profile. The 1'-ethynyl analogue 9 (entry 6)<sup>22</sup> and its corresponding 2-ethylbutyl alanine prodrug 9a (entry 7) were both less active when compared to their respective 1'-CN counterparts (4 and 4a, respectively).

Compound 4 is a C-nucleoside analogue which provides chemical and enzymatic stability toward deglycosylation reactions at the anomeric center. However, alternate base modifications including N-nucleosides were also studied. Interestingly, the corresponding 1'-CN modified adenosine N-analogue 10 (entry 8)<sup>25</sup> was significantly less active toward all viruses, while the 1'-CN modified N-nucleoside pyrimidine 11 (entry 9) retained weak antiviral activity only for RSV and HCV.<sup>26,27</sup> The phosphoramidate prodrug of 1'-CN cytidine 11a (entry 10)<sup>27</sup> did not improve the potency toward EBOV (in HeLa cell assay) or the other viruses tested, presumably due to limitations in metabolism beyond the monophosphate. In general, the potency trends of 1' substitution and nucleobase changes were similar across EBOV, RSV, and HCV, which was in contrast to the trends uncovered with 2' modifications. The 2'-deoxy-2'-fluorine analogue 12 (entry 11)<sup>23</sup> and the 2'-β-methyl analogue 13 (entry 12)<sup>28</sup> both lacked significant

antiviral activity. However, the 2'- $\beta$ -methyl phosphoramidate prodrugs, analogs **13a** and **13b** (entries 13 and 14),<sup>28</sup> respectively, were both potent toward HCV, and only weakly active/inactive toward EBOV and RSV. This result suggests that HCV polymerase is more able to accommodate the 2'- $\beta$ -methyl group compared to the EBOV and RSV polymerases. Taken together with the 1' substitution and nucleobase SAR, the EBOV and RSV polymerases demonstrated similar activity trends, while HCV polymerase was differentiated in SAR at the 2' position.

To interrogate the cell based SAR more rigorously the active NTP metabolite **4tp**<sup>23</sup> was tested toward the viral polymerases (Table 2). The triphosphate **4tp** demonstrated a half-maximal

**Table 2. Inhibition of RSV Polymerase, HCV Polymerase, and Human Polymerases by 4tp**

**4tp**

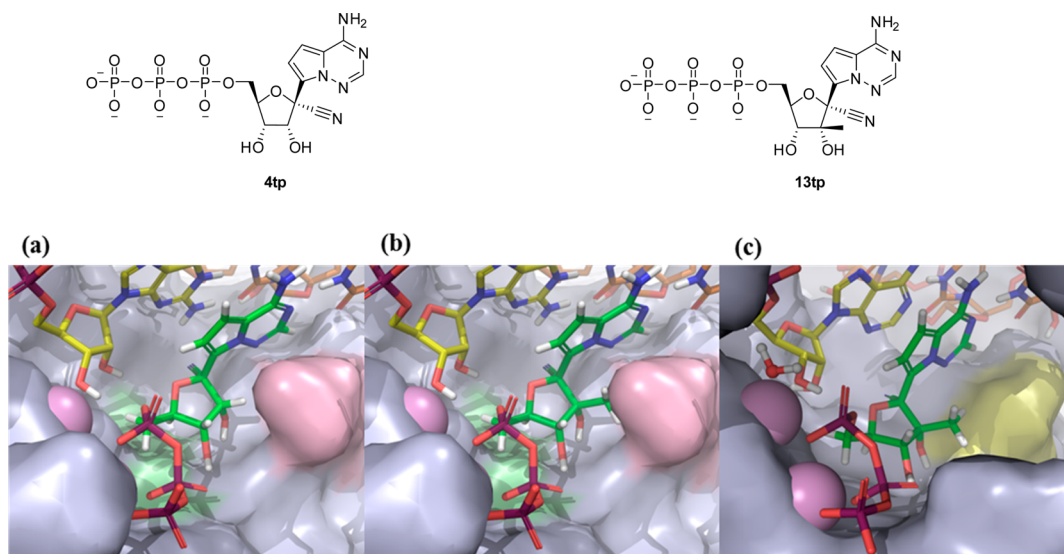
enzyme	<b>4tp</b> IC <sub>50</sub> ( $\mu$ M)	<b>4tp</b> SNI <sup>d</sup> rate (%)
RSV RdRp	1.1	
HCV RdRp	5	
POLRMT	>200	6
RNA Pol II	>200	
DNA Pol $\alpha$	>200	
DNA Pol $\beta$	>200	
DNA Pol $\gamma$	>200	0

<sup>d</sup>SNI = single nucleotide incorporation.

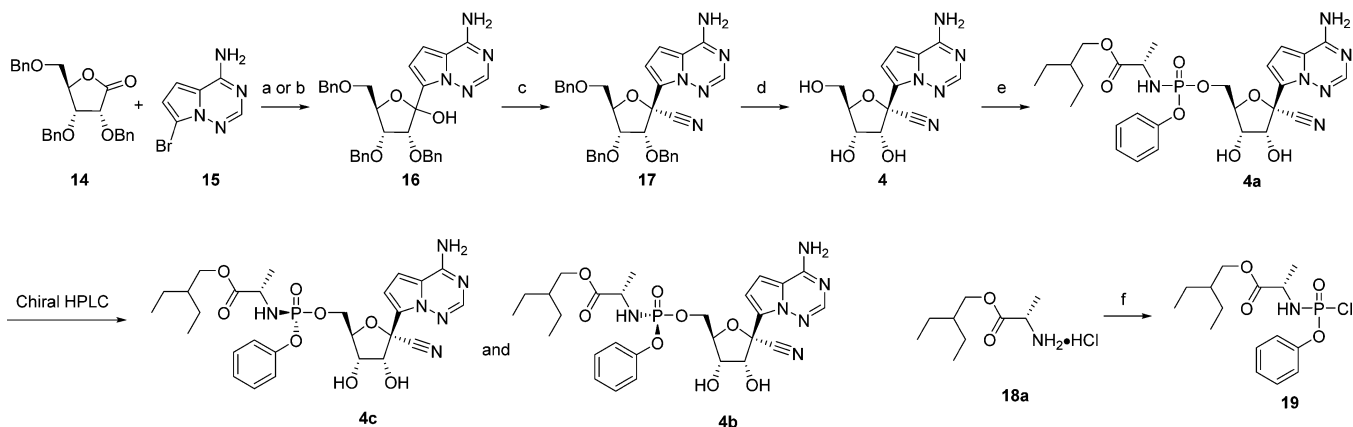
inhibitory concentration (IC<sub>50</sub>) of 1.1  $\mu$ M against the RSV RdRp and 5.0  $\mu$ M against HCV RdRp. The Ebola viral polymerase has to date evaded efforts toward its isolation and

expression, so the intrinsic activity of the active NTP metabolite cannot be directly evaluated. An alternate method for estimating the inhibitory properties of an NTP for its viral target is to measure the NTP levels inside cells following incubation with the parent or prodrug compound at a given concentration and then calculate the NTP levels at the EC<sub>50</sub> measured in the same cells.<sup>17</sup> For example, in a continuous 72 h incubation of 1  $\mu$ M **4a**, the **4tp** levels were measured at 2, 24, 48, and 72 h, and reached a C<sub>max</sub> of 300, 110, and 90 pmol/million cells in macrophages, HMVEC, and HeLa cells lines, respectively. The several-fold difference in maximum **4tp** levels is not unusual and reflects the differences between cells with respect to their ability to break down the prodrug and subsequently metabolize the released monophosphate to the active **4tp**. The average NTP levels over the 72 h incubation of **4a** were then used along with an average cell volume of 2 pL<sup>29</sup> to calculate an estimated half-maximal inhibitory concentration of  $\sim$ 5  $\mu$ M for the intracellular inhibition of EBOV polymerase. This is comparable in potency toward RSV and HCV polymerases supporting the potent antiviral EC<sub>50</sub> data demonstrated for the prodrug mixture **4a** across the three viruses when allowing for cell differences (Table 1). The selective inhibition of the viral polymerases vs host polymerases is considered a key factor in the development of a safe and effective nucleoside antiviral.<sup>30,31</sup> Therefore, **4tp** was evaluated toward several host polymerases and was found to be a weak incorporator toward mitochondrial polymerase (POLRMT) and not a substrate for DNA polymerase  $\gamma$ , as would be expected given the presence of the ribose 2' OH (Table 2). Across the host RNA and DNA polymerases evaluated there was no inhibition up to 200  $\mu$ M (Table 2) demonstrating a high degree of selectivity of **4tp** toward the viral polymerases compared to representative examples of host polymerases.

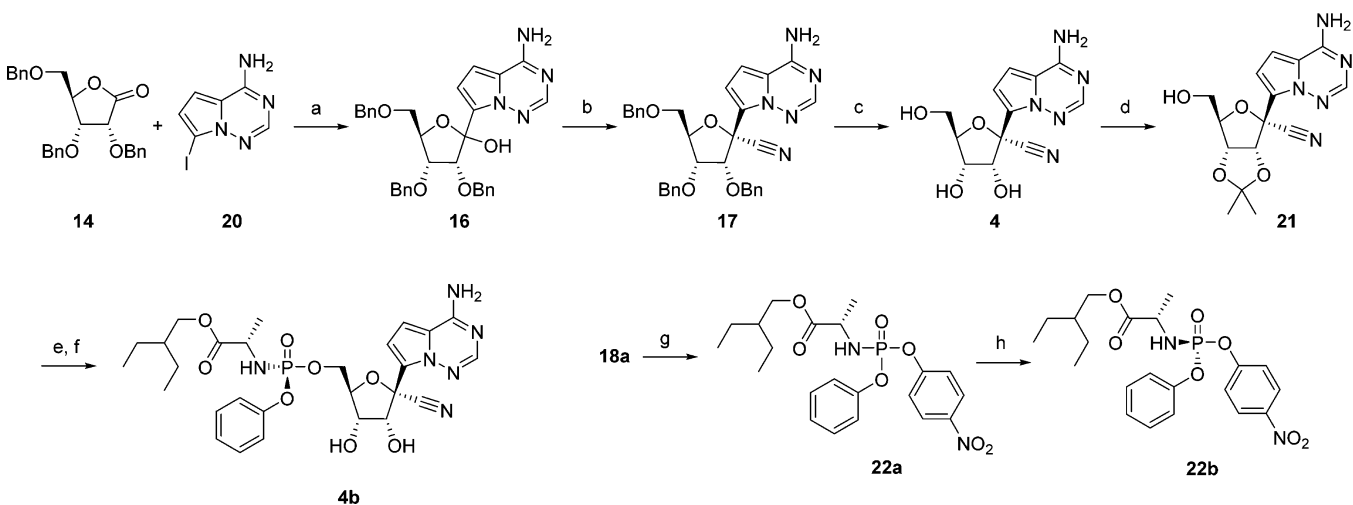
Molecular structure information is not available for the EBOV or RSV polymerases, so modeling of the active sites was performed based on the published structures for HIV and HCV polymerases, together with an analysis of the respective



**Figure 2.** (a) Compound **4tp** modeled into the EBOV polymerase active site. Residue Y636 is highlighted in green surface, sits below the ribose, and corresponds to F704 in RSV. Residue E709 is highlighted in red surface, sits in proximity to the 2'- $\beta$ -H position of the ribose, and corresponds to S282 in HCV. (b) Compound **13tp** modeled into the EBOV polymerase active site. The 2'- $\beta$ -methyl overlaps with residue E709 highlighted in red. (c) Compound **13tp** modeled into the HCV polymerase active site. Residue S282 is highlighted in the yellow surface, and the 2'- $\beta$ -methyl can be accommodated.

Scheme 1. First Generation Synthesis of 4b<sup>a</sup>

<sup>a</sup>Reagents and conditions: (a) *n*-BuLi, (TMS)Cl, THF, -78 °C, 25%; (b) 1,2-bis(chlorodimethylsilyl)ethane, NaH, *n*-BuLi, THF, -78 °C, 60%; (c) (TMS)CN, BF<sub>3</sub>·Et<sub>2</sub>O, CH<sub>2</sub>Cl<sub>2</sub>, -78 °C, 58% (89:11β-17/α); (d) BCl<sub>3</sub>, CH<sub>2</sub>Cl<sub>2</sub>, -78 °C, 74%; (e) 19, NMI, OP(OMe)<sub>3</sub>, 21%; (f) OP(OPh)Cl<sub>2</sub>, Et<sub>3</sub>N, CH<sub>2</sub>Cl<sub>2</sub>, 0 °C, 23%.

Scheme 2. Second Generation Synthesis of 4b<sup>a</sup>

<sup>a</sup>Reagents and conditions: (a) TMSCl, PhMgCl, *i*-PrMgCl·LiCl, THF, -20 °C, 40%; (b) TMSCN, TfOH, TMSOTf, CH<sub>2</sub>Cl<sub>2</sub>, -78 °C, 85%; (c) BCl<sub>3</sub>, CH<sub>2</sub>Cl<sub>2</sub>, -20 °C, 86%; (d) 2,2-dimethoxypropane, H<sub>2</sub>SO<sub>4</sub>, acetone, rt, 90%; (e) 22b, MgCl<sub>2</sub>, (*i*-Pr)<sub>2</sub>NEt, MeCN, 50 °C, 70%; (f) 37% HCl, THF, rt, 69%; (g) OP(OPh)Cl<sub>2</sub>, Et<sub>3</sub>N, CH<sub>2</sub>Cl<sub>2</sub>, -78 °C, then 4-nitrophenol, Et<sub>3</sub>N, 0 °C, 80%; (h) *i*-Pr<sub>2</sub>O, 39%.

sequences.<sup>32</sup> Within the modeled active site of EBOV polymerase the major difference between EBOV and RSV is Y636 (EBOV) compared to F704 (RSV) and the major difference between EBOV and HCV is E709 (EBOV) compared to S282 (HCV). On docking the triphosphate 4tp, the 1'-CN group occupies a pocket formed by residues that are identical between EBOV and RSV, yet very different in HCV (Figure 2a). Nevertheless the 1'-CN analogue retains antiviral potency across these viruses and others<sup>17</sup> suggesting that a pocket exists to accommodate the 1'-CN group in many viral polymerases including other filoviruses.<sup>33</sup> The 2'-β-H of 4tp is in close proximity to E709, and replacement of this group with a 2'-β-methyl (13tp) would be anticipated to interfere with E709 (Figure 2b).<sup>34</sup> However, the 2'-β-methyl can be accommodated by the larger pocket afforded by the smaller S282 residue of HCV (Figure 2c). This suggests the lack of activity for 2'-β-methyl analogs toward EBOV and RSV and retained potency toward HCV is likely due to steric constraints in the polymerase active site. Consistent with the model, EBOV and RSV both have the E709 or equivalent residue, and 13tp

was found to be significantly less active (IC<sub>50</sub> > 30 μM) toward RSV.

The screening and modeling efforts established 4 as the best lead for prodrug optimization. The ability to evaluate prodrugs, especially in vivo, required an efficient synthesis route for both the nucleoside 4 and, preferably, a single prodrug diastereoisomer. Neither was available at the outset, so significant chemistry resources were applied to improve the robustness and scalability of the route along with generation of single prodrug diastereoisomers. The first generation synthesis of 4 and the single Sp phosphoramidate prodrug 4b commenced with a glycosylation reaction via metal-halogen exchange of the bromo-base 15 followed by addition into the ribolactone 14 (Scheme 1). Two conditions were identified to render this desired C-C bond formation. The first condition (a) proceeded through addition of excess *n*-BuLi to a mixture of TMSCl and 15, which was designed to result in lithium-halogen exchange after removal of the acidic 6N protons by silyl protection. Addition of this in situ generated reagent to the ribolactone 14 then afforded 16 in 25% yield.<sup>23,35,36</sup> The

alternative conditions (b) employed sodium hydride and 1,2-bis(chlorodimethylsilyl)ethane for the 6N protection step, followed by lithium–halogen exchange, and addition to the lactone to afford **16** in 60% yield.<sup>22,36</sup>

The efficiency of both conditions was suboptimal as the yields were capricious and highly dependent on the cryogenic temperatures and the rate of *n*-BuLi addition required for the transformation. Furthermore, premature quenching and reduction of lithio base was observed, which was rationalized to be a consequence of deprotonation  $\alpha$  to the lactone under the highly basic conditions. Compound **16** was isolated as a mixture of 1'-isomers, which were taken into the subsequent 1'-cyanation reaction to isolate the major product,  $\beta$ -anomer **17**, by chromatography.<sup>37</sup> Following removal of the three benzyl protecting groups to afford **4**, the diastereomeric mixture of the phosphoramidoyl chloridate prodrug moiety **19** was then coupled to provide **4a** in 21% yield, as an ~1:1 diastereomeric mixture.<sup>23</sup> The two diastereomers were resolved using chiral HPLC to afford the Sp isomer **4b** and Rp isomer **4c**, respectively.<sup>38</sup> While this route initially provided quantities of **4b**, the variability in yields, suboptimal selectivity, frequent use of cryogenic temperatures, and chiral chromatography hindered this route from being suited to larger scales.

The second generation route enabled the diastereoselective synthesis of the single Sp isomer **4b** on scales suitable to advance the compound into preclinical efficacy and toxicity studies (Scheme 2).<sup>17</sup> The glycosylation step employed the iodo-base **20** instead of the bromo base, which enabled a more facile metal–halogen exchange compatible with *i*-PrMgCl·LiCl complex.<sup>39</sup> Treatment with PhMgCl and TMSCl provided 6N protection to remove the acidic protons with a higher degree of control, and addition of *i*-PrMgCl·LiCl followed by the ribolactone **14** at  $-20$  °C afforded the glycosylation product **16** in a 40% yield. The milder reagents and temperature enabled large-scale batches to be carried out with consistent yields. Treatment of **16** with TMSCN, TMSOTf, and TfOH at  $-78$  °C afforded **17** in 85% yield in >95:5 anomeric ratio. The inclusion of TfOH was key to promote the high yield and high selectivity favoring the desired  $\beta$ -anomer. Benzyl deprotection was effected through treatment with BCl<sub>3</sub>, and **4** was readily isolated through crystallization. Acetonide protection of the 2',3'-hydroxyl moieties with 2,2-dimethoxypropane in the presence of H<sub>2</sub>SO<sub>4</sub> afforded **21** in 90% yield. Utilizing the 2',3'-acetonide protection was found to be optimal as the yield of the coupling reaction with the *p*-nitrophenolate 2-ethylbutyl-L-alaninate prodrug mixture **22a** was dramatically improved compared to directly coupling to the unprotected nucleoside **4** (70% vs 40%). In the event, reaction of **21** with the single Sp isomer of the *p*-nitrophenolate prodrug precursor **22b** in the presence of MgCl<sub>2</sub> and Hünig's base efficiently appended the prodrug group in 70% yield as a single Sp isomer. Final deprotection of the acetonide with concentrated HCl in THF afforded **4b** in 69% yield.

The single Sp isomer **22b** of the *p*-nitrophenolate 2-ethylbutyl-L-alaninate prodrug precursor **22a** was prepared through a sequence beginning with exposure of 2-ethylbutyl-L-alanine **18a** to OP(OPh)Cl<sub>2</sub>, followed by 4-nitrophenol, to afford **22a** as a diastereomeric mixture at phosphorus. Importantly, the single Sp isomer **22b** was readily resolved from the mixture in 39% yield through crystallization in diisopropyl ether, a discovery that was paramount for the success of the diastereoselective synthesis of the **4b**.<sup>40</sup> Thus, utilizing the *p*-nitrophenolate 2-ethylbutyl-L-alaninate prodrug

coupling partner **22b** offered a significant advantage over the chloridate **19** in the first generation sequence. Overall the second generation synthesis of **4b** offered the following improvements: (1) milder glycosylation conditions at higher temperature to allow for consistent yields and scalability, (2) higher selectivity and yield for the 1'-cyanation reaction, and (3) a highly efficient coupling sequence of a single Sp prodrug moiety for the diastereoselective synthesis of **4b**. Through this second generation route >200 g was rapidly prepared to support preclinical efficacy and toxicity studies.

The stereochemistry of the *p*-nitrophenolate 2-ethylbutyl-L-alaninate prodrug **22b** and candidate compound **4b** were unambiguously assigned by small molecule X-ray crystallography (Figure 3). In both cases the Sp isomer was established and suggests that the coupling with the nucleoside and reagent follows a S<sub>N</sub>2 type inversion of the phosphorus stereocenter.

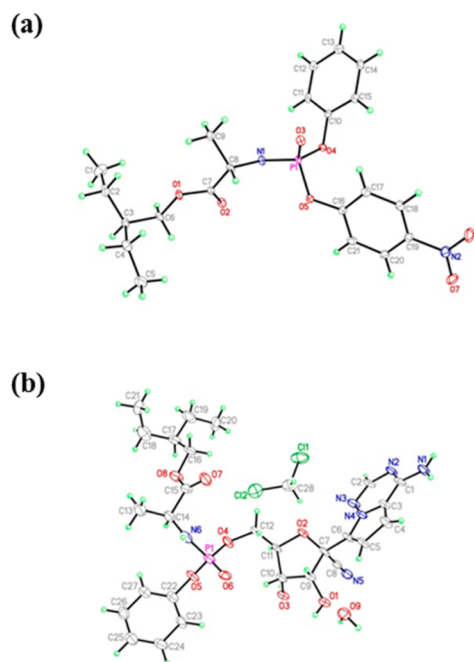
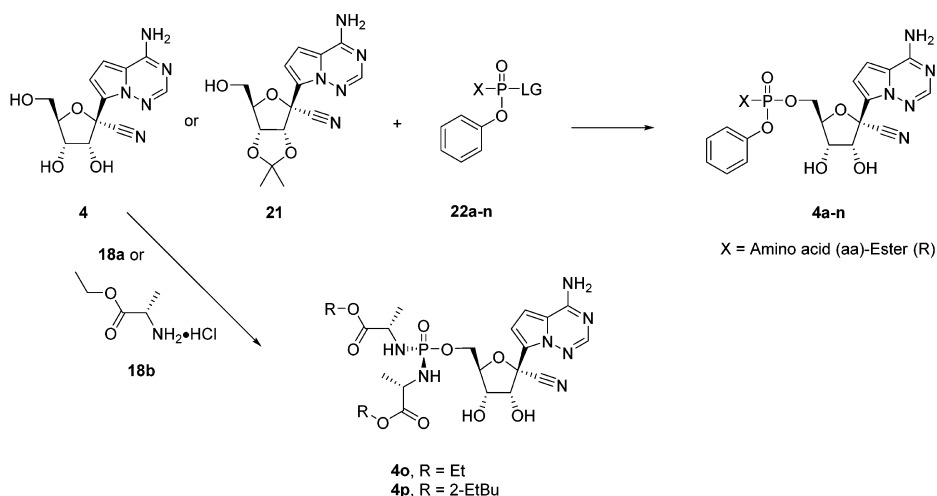


Figure 3. Thermal ellipsoid representations of (a) **22b** and (b) **4b**.

The improved method for preparing **4** enabled many monophosphoramidate and bisphosphoramidate prodrug analogues to be synthesized, the results of which are summarized in Scheme 3. A number of conditions were identified to affect the coupling of the prodrug moieties to **4** or the 2',3'-acetonide protected analogue **21**. The reactions employing **4** proceeded under either Brønsted basic conditions utilizing *t*-BuMgCl or Lewis acidic conditions with MgCl<sub>2</sub> in polar aprotic solvents to afford the desired prodrugs in yields ranging from 10 to 43%. The coupling reaction of the 2',3'-acetonide protected analogue **21** under Lewis acidic conditions followed by in situ acetonide deprotection in general afforded much higher yields ranging from 60 to 70% (analogues **4b** and **4n**). Both the *p*-nitrophenol (PNP) and pentafluorophenol (PFP) prodrug electrophiles were compatible in the coupling reactions and typically achieved comparable yields. The reactions utilizing diastereomeric mixtures of the prodrug electrophiles, **22a,d-h,j,l,n** provided the prodrug products in 1.5–2.6 to 1 diastereomeric ratios (unassigned) at phosphorus. In addition to the monophosphoramidate prodrugs, two bisphosphoramidate pro-

Scheme 3. Prodrug Synthesis



Prodrug <sup>a</sup>	X		LG <sup>c</sup>	Coupling Partner	Conditions	Product	Yield	Isomer Ratio
	ester (R)	aa <sup>b</sup>						
22a	2-EtBu	L-Ala	PNP	4	<i>t</i> -BuMgCl, THF, DMF, rt	4a	43%	2.5 : 1
22b <sup>d</sup>	2-EtBu	L-Ala	PNP	21	MgCl <sub>2</sub> , ( <i>i</i> -Pr) <sub>2</sub> NEt, THF, 50 °C; conc. HCl, 0 °C	4b	69%	Sp Isomer
22d	Et	L-Phe	PNP	4	<i>t</i> -BuMgCl, THF, DMF, rt	4d	34%	2.6 : 1
22e	Et	L-Val	PNP	4	<i>t</i> -BuMgCl, THF, NMP, rt	4e	43%	1.8 : 1
22f	Et	AIB	PNP	4	<i>t</i> -BuMgCl, THF, NMP, 50 °C	4f	25%	1.5 : 1
22g	Et	L-Ala	PNP	4	<i>t</i> -BuMgCl, THF, NMP, rt	4g	24%	2.5 : 1
22h	<i>c</i> -Bu	L-Ala	PNP	4	MgCl <sub>2</sub> , ( <i>i</i> -Pr) <sub>2</sub> NEt, DMF, 50 °C	4h	37%	3 : 2
22i <sup>d</sup>	<i>i</i> -Pr	L-Ala	PNP	4	<i>t</i> -BuMgCl, THF, NMP, 50 °C	4i	38%	Sp Isomer
22j	<i>t</i> -Bu	L-Ala	PNP	4	MgCl <sub>2</sub> , ( <i>i</i> -Pr) <sub>2</sub> NEt, DMF, 50 °C	4j	32%	1.5 : 1
22k <sup>e</sup>	<i>c</i> -Pent	L-Ala	PFP	4	<i>t</i> -BuMgCl, THF, DMF, rt	4k	43%	Single Isomer
22l	3-Pent	L-Ala	PNP	4	MgCl <sub>2</sub> , ( <i>i</i> -Pr) <sub>2</sub> NEt, DMF, 50 °C	4l	42%	1.5 : 1
22m <sup>e</sup>	Neopent	L-Ala	PFP	4	<i>t</i> -BuMgCl, THF, DMF, rt	4m	10%	Single Isomer
22n	2-EtBu	D-Ala	PNP	21	MgCl <sub>2</sub> , ( <i>i</i> -Pr) <sub>2</sub> NEt, THF, 50 °C; conc. HCl, 0 °C	4n	66%	1.1 : 1
18b	Et	L-Ala	NA <sup>f</sup>	4	POCl <sub>3</sub> , PO(OMe) <sub>3</sub> , Et <sub>3</sub> N, rt	4o	16%	NA <sup>f</sup>
18a	2-EtBu	L-Ala	NA <sup>f</sup>	4	POCl <sub>3</sub> , PO(OMe) <sub>3</sub> , Et <sub>3</sub> N, rt	4p	58%	NA <sup>f</sup>

<sup>a</sup>Prodrug is an undetermined mixture of diastereoisomers unless otherwise indicated. <sup>b</sup>aa = amino acid, Ala = alanine, Phe = phenylalanine, AIB = 2-aminoisobutyrate, *c*-Bu = cyclobutyl, *c*-Pent = cyclopentyl, Pent = pentyl, Neopent = neopentyl, 2-EtBu = 2-ethylbutyl, PNP = *p*-nitrophenolate, and PFP = pentafluorophenolate. <sup>c</sup>LG = leaving group. <sup>d</sup>Single Sp isomer. <sup>e</sup>Reagent was a single unassigned isomer at phosphorus. <sup>f</sup>NA = not applicable.

drugs, **4o** and **4p**, were synthesized and evaluated since they avoided the preparation of chiral phosphorus reagents.

The monophosphate prodrugs can improve the potency of the parent nucleosides substantially by delivering the monophosphate into cells and effectively bypassing a rate limiting first phosphorylation step. The phenol and amino acid esters mask the negative charge of the monophosphate group enabling facile passive penetration into the cell. The prodrug breakdown is initiated by intracellular esterases (e.g., carboxy esterase 1 and cathepsin A) that cleave the ester unraveling the carboxylate moiety, which then continues to breakdown to the

monophosphate that serves as the precursor to synthesis of the intracellular NTP.<sup>17</sup>

Prodrugs **4a–p** were evaluated toward EBOV in three cell lines and for human plasma stability (Table 3). In general the antiviral activity trends for EBOV across all three cell lines were similar supporting the efficient conversion of these prodrugs across multiple different cell types. A series of ethyl esters with differing amino acids (entries 2–5) established that the phenylalanine and alanine amino acids were the most promising (Table 3). Given the intended route of administration was intravenous, increasing lipophilicity beyond log *D* ~ 2 was considered a potential issue due to solubility concerns.

Table 3. Antiviral Activity of Prodrugs 4a–p.<sup>a</sup>

entry	compd	ester (R)	aa <sup>b</sup>	EBOV EC <sub>50</sub> HeLa (nM)	EBOV EC <sub>50</sub> HMVEC <sup>c</sup> (nM)	EBOV EC <sub>50</sub> macro <sup>d</sup> (nM)	CC <sub>50</sub> MT4 (μM)	human plasma t <sub>1/2</sub> (min)	log D
1	4			>20000	780	>20000	>57		0.3
2	4d	Et	L-Phe	4380	587	270	15	1584	1.6
3	4e	Et	L-Val	7040	3151		>100	1584	1.2
4	4f	Et	AIB	8470	1585		>100	1584	0.9
5	4g	Et	L-Ala	2425	636		13	1584	0.6
6	4h	c-Bu	L-Ala	420	88		6	815	1.1
7	4i	i-Pr	L-Ala	1845	367	297	21	1561	1.1
8	4j	t-Bu	L-Ala	30410	3790		>100	1584	1.3
9	4k	c-Pent	L-Ala	633	160	120	8.8	1578	1.3
10	4l	3-Pent	L-Ala	1810	845		>100	860	1.6
11	4m	Neopent	L-Ala	168	92		3	700	1.7
12	4a	2-EtBu	L-Ala	170	121	100	2	195	2.1
13	4c	2-EtBu	L-Ala	80	53	111	3	234	2.0
14	4b	2-EtBu	L-Ala	100	53	86	1.7	69	2.1
15	4n	2-EtBu	D-Ala	550	518	729	42	1584	2.1
16	4o	Et	L-Ala	20420	9102		>53		<0.3
17	4p	2-EtBu	L-Ala	970	678		9	507	2.7

<sup>a</sup>Data is at least  $n \geq 2$  unless otherwise reported. <sup>b</sup>aa = Amino Acid, Ala = Alanine, Phe = Phenylalanine, AIB = 2-aminoisobutyrate, c-Bu = cyclobutyl, c-Pent = cyclopentyl, Pent = pentyl, 2-EtBu = 2-ethylbutyl. <sup>c</sup>HMVEC = TERT-immortalized human foreskin microvascular endothelial cells (ATCC-4025). <sup>d</sup>Macro = human macrophages.

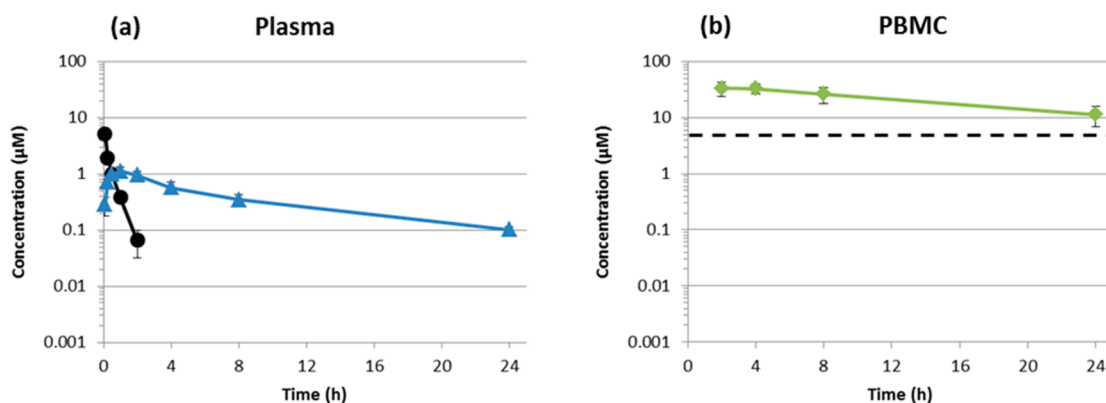


Figure 4. Concentration–time profiles following 10 mg/kg iv single dose slow bolus administration of 4b in Rhesus (mean  $\pm$  SD,  $n = 3$  per time point). (a) Plasma profile of prodrug 4b (black circle) and parent nucleoside 4 (blue triangle). (b) Intracellular concentration of active metabolite 4tp in PBMCs (green diamond) and estimated 4tp EBOV IC<sub>50</sub> = 5 μM (dashed black line).

Therefore, to improve potency the emphasis was placed on the less lipophilic and more commonly used alanine amino acid, with subsequent modification of the ester. Nonproximally branched esters of alanine with increasing log  $D$  ranging from 0.6 to 2.1 (entries 5, 11, and 12) demonstrated increased potency. Esters that contained proximal branching without cyclic motifs e.g. *i*-Pr, *t*-Bu, and 3-pentyl (entries 7, 8, and 10, respectively) were generally less active, consistent with the increased steric hindrance that likely slows the cleavage rate by esterases. For example, the proximally branched 3-pentyl ester 4l (entry 10) has comparable log  $D$  to that of the neopentyl analogue 4m (entry 11) yet much lower potency. In contrast, cyclic butyl and pentyl esters (entries 6 and 9, respectively) are more potent than 4l despite the proximal branching and lower log  $D$ , although the potency in the HeLa cell assay was reduced. The D-Ala 2-EtBu mixture (entry 15) was less potent than the corresponding L-Ala analogue mixture (entry 12), and the two bisphosphoramidate prodrugs (entries 16 and 17) also had reduced activity compared to their monoamidate counterparts (entries 5 and 12, respectively). Thus, based on antiviral

properties across HeLa and HMVEC cells, the most promising monophosphoramidate prodrugs were the neopentyl ester 4m (single undefined isomer) and 2-EtBu ester mixture 4a. The Sp and Rp isomers of 4a (entries 14 and 13, respectively) were separated and found to be similar in potency, but both were marginally more potent than 4m. For the intended iv route of administration, plasma stability was not deemed critical in the selection process provided sufficient stability ( $t_{1/2} > 60$  min) was maintained to allow loading of target cells harboring the virus during drug infusion. The selection of 4b was made based on the high potency across multiple cell lines and the crystalline nature of the Sp prodrug reagent 22b that allowed rapid scale up for efficacy and IND enabling studies of the single Sp isomer 4b.

In vivo efficacy evaluation of 4b was conducted in monkeys since this represented the most relevant animal model of EVD with similar pathophysiology to the actual human disease. In addition, phosphoramidate esters are highly prone to plasma metabolism in rodents on account of high expression of plasma carboxylesterases,<sup>41</sup> thereby excluding pilot efficacy studies in



small animal models. Due to the high first pass hepatic extraction of phosphoramidates, oral administration was also not explored in favor of injectable routes of administration. Moreover, oral delivery in patients acutely infected with EBOV that are demonstrating symptoms of the disease may not be ideal because gastrointestinal symptoms may limit the dose that is effectively absorbed. Intravenous administration of **4b** in rhesus monkeys demonstrated rapid elimination of prodrug and appearance of parent nucleoside in systemic circulation (Figure 4a). However, **4b** also rapidly distributed to peripheral blood mononuclear cells (PBMCs) and triphosphate levels in PBMCs were elevated to a maximum within 2 h (Figure 4b). A dose of 10 mg/kg resulted in an estimated PBMC triphosphate level at 24 h that was several-fold higher than the estimated  $IC_{50}$  of 5  $\mu$ M for EBOV, with a half-life of 14 h similar to that measured in vitro in human macrophages. The long intracellular half-life of **4tp** supported once-daily iv administration in the rhesus efficacy study and in the clinical program.

Preclinical in vivo efficacy for **4b** was conducted in an EBOV-infected rhesus challenge model. The overall strategy was to determine a maximally efficacious dose of **4b** that could be safely administered and to understand whether delayed time of treatment would be effective, a property that was considered critical for the successful clinical application of **4b**. These studies have recently been published in full and will only be summarized here.<sup>17</sup> The starting dose of 3 mg/kg iv was modeled based on the **4tp** levels in rhesus PBMCs following 10 mg/kg iv dosing to have the potential for inhibiting Ebola viral replication in vivo. A correlation of the in vitro antiviral activity and intracellular metabolism described earlier suggested the 3 mg/kg dose would produce **4tp** levels that exceed the estimated  $IC_{50}$  for most of the dosing interval. Compound **4b** was dosed iv at 3 mg/kg on day 0 or day 2 relative to EBOV inoculation, and continued once daily for 12 days. Systemic viremia was reduced and survival out to day 28 postinfection was improved. Animals administered 3 mg/kg **4b**, starting at day 0, had a survival rate of 33% while those initiated on day 3 had a 66% survival at 28 days. These encouraging data were then followed with a second study in which one arm explored dosing initiation on day 3 with 10 mg/kg daily for 12 days to assess whether increased dose compared to the 3 mg/kg result could be more efficacious. Two other arms explored an initial loading dose of 10 mg/kg on day 2 or day 3, followed by 11 3 mg/kg daily maintenance doses. All of the animals in the two arms in which **4b** treatments were initiated on day 3 ( $n = 12$  total) survived through day 28, the end of study. In the daily 10 mg/kg dosed group the effect on viremia was consistently greater than in any of the other groups and was below the limit of quantitation ( $8 \times 10^4$  RNA copies  $mL^{-1}$ ) in four of the six animals on days 5 and 7 relative to the vehicle-treated control in which the geometric mean exceeded  $10^9$  copies  $mL^{-1}$  at these time points. These data established the effectiveness of **4b** in treatment of EVD in NHPs and accelerated its progress into clinical development. In addition to the efficacy studies, distribution studies in cynomolgus monkeys using [ $^{14}C$ ]**4b** at the same effective dose of 10 mg/kg established the presence of drug-related products in the potential sanctuary sites for the virus including testes, epididymis, eyes, and brain.<sup>17</sup> At 4 h postdose, the drug levels in the testes and epididymis exceeded those observed in plasma, and even at 168 h postdose detectable levels of drug-related products were still observed in the testes. Exposure levels in the brain were lower than other tissues, including plasma at 4 h, but were detectable above the

plasma levels at 168 h indicating a long half-life of exposure in brain relative to plasma. These data supported the potential that **4b** treatment may also reduce persistence of virus in these sanctuary sites.

Safety and pharmacokinetics of **4b** administered as once-daily iv infusion were evaluated in single and multiple dose phase 1 clinical trials. No serious adverse effects of the drug were observed. During the course of the phase 1 studies two requests for a compassionate use of **4b** were received. The first case involved a healthcare worker who had survived acute infection but had relapsed with symptoms of acute meningoencephalitis.<sup>42</sup> Ebola virus was detected both systemically in plasma and in cerebrospinal fluid. When treated with monoclonal antibodies, the patient developed adverse reaction and was subsequently treated with supportive therapy and **4b** for a period of 14 days beginning with a dose of 150 mg and then increasing to 225 mg after two daily infusions. No serious adverse effects related to drug were observed. The patient recovered and cleared the virus from both plasma and CNS although without proper control or natural history data to compare, it is not clear whether the antiviral therapy was effective. The second case involved a newborn infant congenitally infected with EBOV and treated with monoclonal antibodies, blood transfusion, and subsequently **4b**.<sup>43</sup> The infant recovered and was eventually declared free of Ebola virus after repeated testing failed to detect viremia. The unprecedented scale of the West African epidemic and the ability to reduce mortality rates through supportive therapy has resulted in many survivors of EVD. The persistence of virus sequelae in survivors in multiple body compartments has now been documented in addition to secondary sexual transmission via virus in genital secretions.<sup>4</sup> This has prompted the initiation of a randomized, blinded, placebo-controlled phase 2 study (PREVAIL IV) which plans to enroll at least 60 adult male survivors to receive either 100 mg of **4b** or placebo once-daily over 5 days to assess the effect of **4b** therapy on the viral shedding in semen.<sup>44</sup> The results of this study could provide the first evidence as to the potential of **4b** to reduce virus replication in humans.

## CONCLUSION

The recent EBOV outbreak prompted the urgent need for antiviral therapeutics for the treatment of EVD. We identified a promising nucleotide therapeutic **4b** through initial screening and subsequent optimization of the prodrug moiety for iv administration. The partnership with government organizations, including CDC and USAMRIID, that generated the screening data and conducted the rhesus efficacy studies was critical to the successful identification of **4b**. Also of importance was the significant chemistry effort that rapidly identified a more efficient route to the parent compound **4** and the ability to prepare, through crystallization of a key reagent, the single Sp phosphorus diastereoisomer **4b** for in vivo model studies. The active triphosphate delivered by the prodrug has low micromolar polymerase activity toward EBOV, high selectivity for the viral polymerase compared to host polymerases, and a long intracellular half-life supporting once-daily administration. Parenteral treatment with **4b** in EBOV infected NHPs at 10 mg/kg over 12 days demonstrated a substantial antiviral effect along with 100% survival. Based on its promising potential, and preliminary safety data from phase 1 studies, regulatory authorities approved the compassionate use of **4b** in two cases including an newborn infant with EVD. Further clinical

data on **4b** is being collected in the phase 2 PREVAIL IV study that aims to assess the ability of **4b** to reduce persistence of EBOV in sanctuary sites of survivors.

## EXPERIMENTAL SECTION

All organic compounds were synthesized at Gilead Sciences, Inc. (Foster City, CA, USA) unless otherwise noted. Commercially available solvents and reagents were used as received without further purification. Nuclear magnetic resonance (NMR) spectra were recorded on a Varian Mercury Plus 400 MHz instrument at room temperature, with tetramethylsilane as an internal standard. Proton nuclear magnetic resonance spectra are reported in parts per million (ppm) on the  $\delta$  scale and are referenced from the residual proton in the NMR solvent (chloroform- $d_1$ ,  $\delta$  7.26; methanol- $d_4$ ,  $\delta$  3.31; DMSO- $d_6$ ,  $\delta$  2.50). Data are reported as follows: chemical shift [multiplicity (s = singlet, d = doublet, t = triplet, q = quartet, p = pentet, sep = septet, m = multiplet, br = broad, app = apparent); coupling constants ( $J$ ) in hertz; integration. Carbon-13 nuclear magnetic resonance spectra are reported in parts per million on the  $\delta$  scale and are referenced from the carbon resonances of the solvent (chloroform- $d_1$ ,  $\delta$  77.16, methanol- $d_4$ ,  $\delta$  49.15; DMSO- $d_6$ ,  $\delta$  39.52). Data are reported as follows: chemical shift. No special nomenclature is used for equivalent carbons. Phosphorus-31 nuclear magnetic resonance spectra are reported in parts per million on the  $\delta$  scale. Data are reported as follows: chemical shift [multiplicity (s = singlet, d = doublet, t = triplet); coupling constants ( $J$ ) in hertz. No special nomenclature is used for equivalent phosphorus resonances. Analytical thin-layer chromatography was performed using Merck KGaA silica gel 60 F<sub>254</sub> glass plates with UV visualization. Preparative normal phase silica gel chromatography was carried out using a Teledyne ISCO CombiFlash Companion instrument with silica gel cartridges. Purities of the final compounds were determined by high-performance liquid chromatography (HPLC) and were greater than 95% unless otherwise noted. HPLC conditions to assess purity were as follows: Agilent 1100 Series HPLC, Phenomenex Kinetex C18; 2.6  $\mu$ m, 100 Å, 100  $\times$  4.6 mm<sup>2</sup> column, 2–98% gradient of 0.1% trifluoroacetic acid in water, and 0.1% trifluoroacetic acid in acetonitrile; flow rate, 1.5 mL/min; acquisition time, 8.5 min; wavelength, UV 214 and 254 nm. High-resolution mass spectrometry (HRMS) was performed on an Agilent model 6230 accurate mass time of flight mass spectrometer featuring Agilent Jet Stream Thermal Focusing Technology, with an Agilent 1200 Rapid Resolution HPLC. HRMS chromatography was performed using an Agilent Zorbax Eclipse Plus C18 RRHD 1.8  $\mu$ m, 2.1  $\times$  50 mm<sup>2</sup> column at 30 °C, with a 10–90% gradient of 0.05% trifluoroacetic acid in water and 0.05% trifluoroacetic acid in acetonitrile. LC-MS (MS) was conducted on a Thermo Finnigan MSQ Std. using electrospray positive and negative [ $M + 1$ ]<sup>+</sup> and [ $M - 1$ ]<sup>-</sup>, and a Dionex Summit HPLC System (model P680A HPG) equipped with a Gemini 5  $\mu$  C18 110A column (30 mm  $\times$  4.60 mm), eluting with 0.05% formic acid in 1% acetonitrile/water and 0.05% formic acid in 99% acetonitrile/water. Optical rotations were recorded on a Jasco P-2000 polarimeter.

The synthesis, characterization data, and associated references for the following compounds are provided in the [Supporting Information](#): **4**, **4a**, **7–11**, **9a**, **11a**, **12–13**, **13a**, **13b**, **4tp**, **13tp**, **16–17**, **18a**, **19**, **21**, and **22a–n**.

**(S)-2-Ethylbutyl 2-(((S)-(((2R,3S,4R,5R)-5-(4-Aminopyrrolo[2,1-f][1,2,4]triazin-7-yl)-5-cyano-3,4-dihydroxytetrahydrofuran-2-yl)methoxy)(phenoxy)phosphoryl)amino)propanoate (4b)**. Compound **4b** was prepared from **4** and **22b** as described previously.<sup>17</sup> <sup>1</sup>H NMR (400 MHz, methanol- $d_4$ ):  $\delta$  7.86 (s, 1H), 7.33–7.26 (m, 2H), 7.21–7.12 (m, 3H), 6.91 (d,  $J$  = 4.6 Hz, 1H), 6.87 (d,  $J$  = 4.6 Hz, 1H), 4.79 (d,  $J$  = 5.4 Hz, 1H), 4.43–4.34 (m, 2H), 4.28 (ddd,  $J$  = 10.3, 5.9, 4.2 Hz, 1H), 4.17 (t,  $J$  = 5.6 Hz, 1H), 4.02 (dd,  $J$  = 10.9, 5.8 Hz, 1H), 3.96–3.85 (m, 2H), 1.49–1.41 (m, 1H), 1.35–1.27 (m, 8H), 0.85 (t,  $J$  = 7.4 Hz, 6H). <sup>13</sup>C NMR (100 MHz, methanol- $d_4$ ):  $\delta$  174.98, 174.92, 157.18, 152.14, 152.07, 148.27, 130.68, 126.04, 125.51, 121.33, 121.28, 117.90, 117.58, 112.29, 102.60, 84.31, 84.22, 81.26, 75.63, 71.63, 68.10, 67.17, 67.12, 51.46, 41.65, 24.19, 20.56, 20.50, 11.33, 11.28. <sup>31</sup>P NMR (162 MHz, methanol- $d_4$ ):  $\delta$  3.66 (s).

HRMS ( $m/z$ ): [ $M$ ]<sup>+</sup> calcd for C<sub>27</sub>H<sub>35</sub>N<sub>6</sub>O<sub>8</sub>P, 602.2254; found, 602.2274. [ $\alpha$ ]<sub>D</sub><sup>21</sup> – 21 (c 1.0, MeOH).

**(S)-2-Ethylbutyl 2-(((R)-(((2R,3S,4R,5R)-5-(4-Aminopyrrolo[2,1-f][1,2,4]triazin-7-yl)-5-cyano-3,4-dihydroxytetrahydrofuran-2-yl)methoxy)(phenoxy)phosphoryl)amino)propanoate (4c)**. Compound **4c** was prepared from **4a** by chiral chromatography. Compound **4a** was dissolved in acetonitrile. The resulting solution was loaded onto a Lux Cellulose-2 chiral column, equilibrated in acetonitrile, and eluted with isocratic acetonitrile/methanol (95:5 (v/v)). The first eluting compound was the Rp diastereomer **4c**, and the second eluting compound was the Sp diastereomer **4b**. <sup>1</sup>H NMR (400 MHz, methanol- $d_4$ ):  $\delta$  8.05 (s, 1H), 7.36 (d,  $J$  = 4.8 Hz, 1H), 7.29 (br t,  $J$  = 7.8 Hz, 2H), 7.19–7.13 (m, 3H), 7.11 (d,  $J$  = 4.8 Hz, 1H), 4.73 (d,  $J$  = 5.2 Hz, 1H), 4.48–4.38 (m, 2H), 4.37–4.28 (m, 1H), 4.17 (t,  $J$  = 5.6 Hz, 1H), 4.08–3.94 (m, 2H), 3.94–3.80 (m, 1H), 1.48 (sep,  $J$  = 12.0, 6.1 Hz, 1H), 1.34 (p,  $J$  = 7.3 Hz, 4H), 1.29 (d,  $J$  = 7.2 Hz, 3H), 0.87 (t,  $J$  = 7.4 Hz, 6H). <sup>31</sup>P NMR (162 MHz, methanol- $d_4$ ):  $\delta$  3.71 (s). MS  $m/z$ : 603.1 [ $M + 1$ ]. [ $\alpha$ ]<sub>D</sub><sup>21</sup> – 46 (c 1.0, MeOH).

**(2S)-Ethyl-2-(((S)-(((2R,3S,4R,5R)-5-(4-aminopyrrolo[2,1-f][1,2,4]triazin-7-yl)-5-cyano-3,4-dihydroxytetrahydrofuran-2-yl)methoxy)(phenoxy)phosphoryl)amino)-3-phenylpropanoate (4d)**. Compound **4** (0.030 g, 0.103 mmol) was dissolved in DMF (1 mL), and then THF (0.5 mL) was added. *t*-BuMgCl (1 M/THF, 154.5  $\mu$ L, 0.154  $\mu$ mol) was added to the reaction in a dropwise manner with vigorous stirring. The resulting white slurry was stirred at rt for about 30 min. A solution of compound **22d** (0.058 g, 0.124 mmol) in THF (1 mL) was added in a dropwise manner to the reaction at rt. The reaction progress was monitored by LC-MS. When the reaction progressed to 50% conversion, the reaction was cooled in an ice bath and quenched with glacial acetic acid (70  $\mu$ L). The reaction was concentrated and the crude residue was purified by reverse phase preparatory HPLC to afford compound **4d** (22 mg, 34%, as a 2.6:1 mixture of diastereomers at phosphorus). <sup>1</sup>H NMR (400 MHz, DMSO- $d_6$ ):  $\delta$  7.91 (d,  $J$  = 4 Hz, 1H), 7.90 (br s, 2H), 7.09–7.30 (m, 8H), 7.01 (t,  $J$  = 8.2 Hz, 2H), 6.89 (d,  $J$  = 4.4 Hz, 1H), 6.82 (t,  $J$  = 4.4 Hz, 1H), 6.27 (m, 1H), 6.14 (m, 1H), 5.34 (m, 1H), 4.62 (t,  $J$  = 5.6 Hz, 1H), 4.15 (m, 1H), 4.01–3.78 (m, 6H), 2.92 (m, 1H), 2.78 (m, 1H), 1.04 (m, 3H). <sup>31</sup>P NMR (162 MHz, DMSO- $d_6$ )  $\delta$  3.69 (s), 3.34 (s). MS  $m/z$  = 623.0 [ $M + 1$ ].

**(2S)-Ethyl 2-(((S)-(((2R,3S,4R,5R)-5-(4-Aminopyrrolo[2,1-f][1,2,4]triazin-7-yl)-5-cyano-3,4-dihydroxytetrahydrofuran-2-yl)methoxy)(phenoxy)phosphoryl)amino)-3-methylbutanoate (4e)**. Compound **4** (0.040 g, 0.14 mmol) was dissolved in NMP (1.5 mL) and then THF (0.25 mL) was added. This solution was cooled in an ice bath and *t*-BuMgCl (1M/THF, 425.7  $\mu$ L, 0.426  $\mu$ mol) was added in a dropwise manner with vigorous stirring. The ice bath was removed, and the resulting white slurry was stirred at rt for about 15 min. A solution of compound **22e** (0.081 g, 0.192 mmol) in THF (0.5 mL) was added in a dropwise manner to the reaction at rt. The reaction progress was monitored by LC-MS. When the reaction progressed to 50% conversion, the reaction was cooled in an ice bath and quenched with glacial acetic acid (70  $\mu$ L). The reaction was concentrated and crude residue was semipurified from the residue by reverse phase HPLC. The semipure material was further purified by silica gel column chromatography (eluent, 100% EtOAc ramping to 10% MeOH in EtOAc) to afford compound **4e** (0.034 g, 43% as a 1.8:1 mixture of diastereomers). <sup>1</sup>H NMR (400 MHz, DMSO- $d_6$ ):  $\delta$  7.91 (d,  $J$  = 1.6 Hz, 1H), 7.88 (br s, 2H), 7.32 (m, 2H), 7.15 (m, 3H), 6.90 (t,  $J$  = 4.2 Hz, 1H), 6.84 (d,  $J$  = 4.8 Hz, 1H), 6.26 (dd,  $J$  = 13.4, 6.2 Hz, 1H), 5.87 (q,  $J$  = 11.2 Hz, 1H), 5.35 (m, 1H), 4.64 (m, 1H), 4.25 (m, 2H), 4.15–3.93 (m, 4H), 3.45 (m, 1H), 1.87 (m, 1H), 1.16–1.09 (m, 3H), 0.83–0.70 (m, 6H). <sup>31</sup>P NMR (162 MHz, DMSO- $d_6$ ):  $\delta$  4.59 (s), 4.47 (s). MS  $m/z$  = 575.02 [ $M + 1$ ].

**Ethyl 2-(((S)-(((2R,3S,4R,5R)-5-(4-Aminopyrrolo[2,1-f][1,2,4]triazin-7-yl)-5-cyano-3,4-dihydroxytetrahydrofuran-2-yl)methoxy)(phenoxy)phosphoryl)amino)-2-methylpropanoate (4f)**. Compound **4** (66 mg, 0.23 mmol) was dissolved in NMP (2.0 mL) and the mixture was cooled to about 0 °C. *t*-BuMgCl (1.0 M in THF, 0.34 mL, 0.34 mmol) was then added and the resulting mixture was stirred at 0 °C for about 30 min. A solution of compound **22f** (139 mg, 0.34 mmol) in THF (1.0 mL) was then added, and the reaction

mixture was heated to about 50 °C. After about 2 h, the reaction was cooled to rt and quenched with acetic acid and methanol. The resulting mixture was concentrated under reduced pressure and purified by preparatory reverse phase HPLC to afford compound **4f** (32 mg, 25% as a 1.5:1 mixture of diastereomers). <sup>1</sup>H NMR (400 MHz, DMSO-*d*<sub>6</sub>): δ 7.89 (m, 3H), 7.31 (q, *J* = 8.1 Hz, 2H), 7.22–7.05 (m, 3H), 6.87 (d, *J* = 4.5 Hz, 1H), 6.80 (d, *J* = 4.5 Hz, 1H), 6.27 (d, *J* = 11.7 Hz, 1H), 5.81 (d, *J* = 9.7 Hz, 1H), 5.35 (d, *J* = 5.6 Hz, 1H), 4.64 (dt, *J* = 9.0, 5.6 Hz, 1H), 4.24 (m, 2H), 4.11 (m, 1H), 4.04–3.90 (m, 3H), 1.39–1.23 (m, 6H), 1.10 (t, *J* = 7.1, 3H). <sup>31</sup>P NMR (162 MHz, DMSO-*d*<sub>6</sub>): δ 2.45, 2.41. MS *m/z* = 561.03 [*M* + 1].

**Ethyl (((2*R*,3*S*,4*R*,5*R*)-5-(4-Aminopyrrolo[2,1-*f*][1,2,4]triazin-7-yl)-5-cyano-3,4-dihydroxytetrahydrofuran-2-yl)methoxy)(phenoxy)phosphoryl)-L-alaninate (**4g**). Compound **4** (50 mg, 0.17 mmol) was dissolved in NMP–THF (1:1 mL) and cooled with an ice bath. *t*-BuMgCl (1.0 M in THF, 0.257 mL, 0.257 mmol) was then added over about 5 min. The resulting mixture was allowed to warm to rt and was stirred for about 30 min. Then a solution of compound **22g** (74.6 mg, 0.189 mmol) in THF (2 mL) was added. After about 30 min, the reaction mixture was purified by preparatory reverse phase HPLC. Fractions containing the desired product were further purified with silica gel chromatography (eluent: 0–20% methanol in dichloromethane) to afford compound **4g** (23 mg, 24% as a 2.5:1 mixture of diastereomers). <sup>1</sup>H NMR (400 MHz, methanol-*d*<sub>4</sub>): δ 7.76 (d, *J* = 6.0 Hz, 1H), 7.25–7.14 (m, 2H), 7.11–6.99 (m, 3H), 6.87–6.72 (m, 2H), 4.70 (d, *J* = 5.4 Hz, 1H), 4.39–4.24 (m, 2H), 4.20 (dddd, *J* = 9.7, 7.9, 5.1, 2.8 Hz, 1H), 4.10 (dt, *J* = 12.8, 5.5 Hz, 1H), 4.06–3.91 (m, 2H), 3.72 (ddq, *J* = 14.3, 9.3, 7.1 Hz, 1H), 1.17 (dd, *J* = 7.1, 1.0 Hz, 1H), 1.14–1.06 (m, 5H). <sup>31</sup>P NMR (162 MHz, methanol-*d*<sub>4</sub>): δ 3.73, 3.68. MS *m/z* = 547 [*M* + 1].**

**(2*S*)-Cyclobutyl 2-((((2*R*,3*S*,4*R*,5*R*)-5-(4-Aminopyrrolo[2,1-*f*][1,2,4]triazin-7-yl)-5-cyano-3,4-dihydroxytetrahydrofuran-2-yl)methoxy)(phenoxy)phosphoryl)amino)propanoate (**4h**). Compound **4** (58 mg, 0.20 mmol) was mixed with compound **22h** (101 mg, 0.240 mmol) in 2 mL of anhydrous DMF. Magnesium chloride (42 mg, 0.44 mmol) was added in one portion. The reaction mixture was heated to about 50 °C. *N,N*-Diisopropylethylamine (87 μL, 0.5 mmol) was added, and the reaction was stirred for about 2 h at about 50 °C. The reaction mixture was cooled to room temperature, was diluted with ethyl acetate, and was washed with 5% aqueous citric acid solution followed by saturated aqueous sodium chloride solution. The organic layer was then dried over anhydrous sodium sulfate and concentrated under reduced pressure. The crude residue was purified with silica gel column (eluent, 0–5% methanol in dichloromethane) to afford compound **4h** (42 mg, 37% yield, as a 3:2 mixture of diastereomers). <sup>1</sup>H NMR (400 MHz, methanol-*d*<sub>4</sub>): δ 7.85 (m, 1H), 7.34–7.22 (m, 2H), 7.22–7.08 (m, 3H), 6.94–6.84 (m, 2H), 4.95–4.85 (m, 1H), 4.79 (m, 1H), 4.46–4.34 (m, 2H), 4.34–4.24 (m, 1H), 4.19 (m, 1H), 3.81 (m, 1H), 2.27 (m, 2H), 2.01 (m, 2H), 1.84–1.68 (m, 1H), 1.62 (m, 1H), 1.30–1.16 (m, 3H). <sup>31</sup>P NMR (162 MHz, methanol-*d*<sub>4</sub>): δ 3.70, 3.65. MS *m/z* = 573.0 [*M* + 1].**

**(*S*)-Isopropyl 2-((((2*R*,3*S*,4*R*,5*R*)-5-(4-Aminopyrrolo[2,1-*f*][1,2,4]triazin-7-yl)-5-cyano-3,4-dihydroxytetrahydrofuran-2-yl)methoxy)(phenoxy)phosphoryl)amino)propanoate (**4i**). Compound **4** (60.0 mg, 206 μmol) was dissolved in NMP (0.28 mL). THF (0.2 mL) was added followed by *tert*-butyl magnesium chloride (1.0 M solution in tetrahydrofuran, 0.309 mL) at rt under an argon atmosphere. After 20 min, a solution of compound **22i** (81 mg, 206 μmol) in THF (0.2 mL) was added, and the resulting mixture was warmed to about 50 °C. After 3 h, the reaction mixture was allowed to cool to rt and was purified directly by preparatory HPLC to afford compound **4i** (44 mg, 38% as a single diastereomer). <sup>1</sup>H NMR (400 MHz, methanol-*d*<sub>4</sub>): δ 7.86 (s, 1H), 7.34–7.26 (m, 2H), 7.21–7.12 (m, 3H), 6.91 (d, *J* = 4.6 Hz, 1H), 6.87 (d, *J* = 4.6 Hz, 1H), 4.92 (sep, *J* = 6.3 Hz, 1H), 4.80 (d, *J* = 5.4 Hz, 1H), 4.43–4.34 (m, 1H), 4.33–4.24 (m, 1H), 4.18 (t, *J* = 5.6 Hz, 1H), 3.82 (dq, *J* = 9.7, 7.1 Hz, 2H), 1.27 (dd, *J* = 7.1, 1.0 Hz, 3H), 1.18 (dd, *J* = 6.3, 4.8 Hz, 6H). <sup>31</sup>P NMR (162 MHz, methanol-*d*<sub>4</sub>): δ 3.72 (s). MS *m/z* = 561.11 [*M* + 1].**

***tert*-Butyl (((2*R*,3*S*,4*R*,5*R*)-5-(4-Aminopyrrolo[2,1-*f*][1,2,4]triazin-7-yl)-5-cyano-3,4-dihydroxytetrahydrofuran-2-yl)methoxy)(phenoxy)phosphoryl)-L-alaninate (**4j**). To a mixture of**

intermediate **4** (80 mg, 0.28 mmol), intermediate **22j** (174 mg, 0.41 mmol), and MgCl<sub>2</sub> (39 mg, 0.41 mmol) in DMF (4 mL) was added *N,N*-diisopropylethylamine (0.12 mL, 0.69 mmol) dropwise at room temperature. The reaction mixture was stirred at 50 °C for 1 h and was cooled to rt. The resulting mixture was concentrated under reduced pressure to approximately 2 mL volume and was purified by reverse phase preparative HPLC. Fractions containing the desired product were combined and further purified by silica gel column chromatography (eluent, 0–20% methanol in methylene chloride) to afford compound **4j** (51 mg, 32%, 1.5:1 diastereomeric mixture). <sup>1</sup>H NMR (400 MHz, methanol-*d*<sub>4</sub>): δ 7.86 (s, 0.4H), 7.84 (s, 0.6H), 7.28 (m, 2H), 7.21–7.10 (m, 3H), 6.96–6.83 (m, 2H), 4.79 (m, 1H), 4.46–4.34 (m, 2H), 4.28 (m, 1H), 4.22–4.13 (m, 1H), 3.81–3.64 (m, 1H), 1.40 (m, 9H), 1.22 (m, 3H). <sup>31</sup>P NMR (162 MHz, methanol-*d*<sub>4</sub>): δ 3.79 (s). MS *m/z* = 575 [*M* + 1].

**(2*S*)-Cyclopentyl 2-((((2*R*,3*S*,4*R*,5*R*)-5-(4-Aminopyrrolo[2,1-*f*][1,2,4]triazin-7-yl)-5-cyano-3,4-dihydroxytetrahydrofuran-2-yl)methoxy)(phenoxy)phosphoryl)amino)propanoate (**4k**). Compound **4** (100 mg, 0.34 mmol) was dissolved in THF (2 mL) and cooled under an ice water bath. Then 1 M *t*-BuMgCl (0.52 mL, 0.77 mmol) was added dropwise slowly. The resulting mixture was stirred for about 30 min at rt. Then compound **22k** (247 mg, 0.52 mmol) in THF (2 mL) was added over about 5 min and the resulting mixture was stirred for about 24 h at rt. The resulting mixture was diluted with ethyl acetate, cooled under ice–water bath, treated with aqueous NaHCO<sub>3</sub> (2 mL), washed with brine, dried with sodium sulfate, and concentrated under reduced pressure. The resulting mixture was purified by silica gel column chromatography (eluent, 0–20% methanol in dichloromethane) followed by reverse phase preparatory HPLC to afford compound **4k** (47 mg, 23% as a 27:1 mixture of diastereomers). <sup>1</sup>H NMR (400 MHz, methanol-*d*<sub>4</sub>): δ 7.85 (s, 1H), 7.33–7.22 (m, 2H), 7.14 (tdd, *J* = 7.6, 2.1, 1.1 Hz, 3H), 6.95–6.87 (m, 2H), 5.13–5.00 (m, 1H), 4.78 (d, *J* = 5.4 Hz, 1H), 4.48–4.35 (m, 2H), 4.30 (ddd, *J* = 10.6, 5.7, 3.6 Hz, 1H), 4.19 (t, *J* = 5.4 Hz, 1H), 3.78 (dq, *J* = 9.2, 7.1 Hz, 1H), 1.81 (dtd, *J* = 12.5, 5.9, 2.4 Hz, 2H), 1.74–1.49 (m, 6H), 1.21 (dd, *J* = 7.1, 1.2 Hz, 3H). MS *m/z* = 587 [*M* + 1].**

**Pentan-3-yl (((2*R*,3*S*,4*R*,5*R*)-5-(4-Aminopyrrolo[2,1-*f*][1,2,4]triazin-7-yl)-5-cyano-3,4-dihydroxytetrahydrofuran-2-yl)methoxy)(phenoxy)phosphoryl)-L-alaninate (**4l**). To a mixture of compound **4** (80 mg, 0.28 mmol), **22l** (170 mg, 0.39 mmol), and MgCl<sub>2</sub> (39 mg, 0.41 mmol) in DMF (4 mL) was added *N,N*-diisopropylethylamine (0.12 mL, 0.69 mmol) dropwise at rt. The resulting mixture was stirred at 50 °C for 1 h, concentrated to approximately 2 mL volume, and purified by reverse phase preparative HPLC to afford compound **4l** (68 mg, 42%, 1.5:1 diastereomeric mixture). <sup>1</sup>H NMR (400 MHz, methanol-*d*<sub>4</sub>): δ 7.86 (s, 0.4 H), 7.85 (s, 0.6 H), 7.33–7.23 (m, 2H), 7.21–7.08 (m, 3H), 6.95–6.84 (m, 2H), 4.79 (m, 1H), 4.69 (m, 1H), 4.47–4.34 (m, 2H), 4.34–4.24 (m, 1H), 4.19 (m, 1H), 3.85 (m, 1H), 1.64–1.42 (m, 4H), 1.29 (dd, *J* = 7.0, 1.1 Hz, 1.1 H), 1.23 (dd, *J* = 7.2, 1.3 Hz, 1.9H), 0.91–0.76 (m, 6H). <sup>31</sup>P NMR (162 MHz, methanol-*d*<sub>4</sub>): δ 3.71, 3.69. MS *m/z* = 589 [*M* + 1].**

**(*S*)-Neopentyl 2-((((2*R*,3*S*,4*R*,5*R*)-5-(4-Aminopyrrolo[2,1-*f*][1,2,4]triazin-7-yl)-5-cyano-3,4-dihydroxytetrahydrofuran-2-yl)methoxy)(phenoxy)phosphoryl)amino)propanoate (**4m**). Compound **4** (100 mg, 0.34 mmol) was dissolved in THF (2 mL) and cooled under ice water bath. Then 1 M *t*-BuMgCl (0.52 mL, 0.77 mmol) was added dropwise slowly. The resulting mixture was stirred for 30 min at room temperature. Then compound **22m** (248 mg, 0.52 mmol) was added over 5 min, and the resulting mixture was stirred for 24 h at room temperature, diluted with EtOAc, cooled under ice–water bath, treated with aqueous NaHCO<sub>3</sub> (2 mL), washed with brine, dried with sodium sulfate, and concentrated in vacuo. The resulting mixture was purified by silica gel column chromatography (MeOH 0 to 20% in DCM) and prep-HPLC (acetonitrile 10 to 80% in water) to give compound **4m** (12 mg, 10% as a single diastereomer). <sup>1</sup>H NMR (400 MHz, methanol-*d*<sub>4</sub>): δ 7.86 (s, 1H), 7.36–7.24 (m, 2H), 7.23–7.10 (m, 3H), 6.96–6.85 (m, 2H), 4.78 (d, *J* = 5.4 Hz, 1H), 4.38 (tdd, *J* = 10.0, 4.9, 2.5 Hz, 2H), 4.32–4.24 (m, 1H), 4.17 (t, *J* = 5.6 Hz, 1H),**

3.91 (dq,  $J = 9.8$ , 7.1 Hz, 1H), 3.81 (d,  $J = 10.5$  Hz, 1H), 3.69 (d,  $J = 10.5$  Hz, 1H), 1.31 (dd,  $J = 7.2$ , 1.1 Hz, 3H), 0.89 (s, 9H). MS  $m/z = 589$  [ $M + 1$ ]<sup>+</sup>

**2-Ethylbutyl (((2*R*,3*S*,4*R*,5*R*)-5-(4-Aminopyrrolo[2,1-*f*]-[1,2,4]triazin-7-yl)-5-cyano-3,4-dihydroxytetrahydrofuran-2-yl)methoxy)(phenoxy)phosphoryl)-D-alaninate (4n).** Compound **21** (50 mg, 0.15 mmol) was dissolved in anhydrous tetrahydrofuran (5 mL) and stirred under atmospheric argon. Compound **22n** (75 mg, 0.17 mmol) was added followed by magnesium chloride (21 mg, 0.23 mmol), and the reaction was warmed to 50 °C and stirred for 30 min. *N,N*-diisopropylethylamine (65.0  $\mu$ L, 0.375 mmol) was added dropwise, and the reaction mixture was stirred for 3 h at 50 °C. The reaction mixture was then cooled in an ice bath, and 12 N HCl(aq) (175  $\mu$ L) was added dropwise. The ice bath was removed, and the reaction mixture was stirred at rt for 4 h. The reaction mixture was diluted with ethyl acetate (15 mL) and cooled in an ice bath. Aqueous 1 N NaOH solution was added slowly to give pH of 10. The organic layer was then washed with 5% aqueous sodium carbonate solution and then saturated aqueous sodium chloride solution. The organic layer was then dried over anhydrous sodium sulfate and concentrated under reduced pressure. The crude residue was purified with silica gel column chromatography (eluent, 0–10% methanol in dichloromethane) to afford compound **4n** (60 mg, 66% yield as a 1.1:1 diastereomeric mixture). <sup>1</sup>H NMR (400 MHz, methanol-*d*<sub>4</sub>):  $\delta$  7.87–7.83 (m, 1H), 7.37–7.22 (m, 2H), 7.22–7.04 (m, 3H), 6.96–6.79 (m, 2H), 4.82–4.75 (m, 1H), 4.45–4.23 (m, 3H), 4.18 (m, 1H), 4.06–3.85 (m, 3H), 1.52–1.38 (m, 1H), 1.38–1.24 (m, 7H), 0.85 (m, 6H). <sup>31</sup>P NMR (162 MHz, methanol-*d*<sub>4</sub>):  $\delta$  3.87, 3.55. MS  $m/z = 603.1$  [ $M + 1$ ].

**(2*S*,2'*S*)-Diethyl 2,2'-(((2*R*,3*S*,4*R*,5*R*)-5-(4-Aminopyrrolo[1,2-*f*]-[1,2,4]triazin-7-yl)-5-cyano-3,4-dihydroxytetrahydrofuran-2-yl)methoxy)phosphoryl)bis(azanediyl)dipropionate (4o).** Compound **4** (14.6 mg, 0.05 mmol) was dissolved in anhydrous trimethyl phosphate (0.5 mL) and stirred under N<sub>2</sub>(g) at rt. POCl<sub>3</sub> (9.2  $\mu$ L, 0.1 mmol) was added, and the mixture stirred for about 60 min. Alanine ethyl ester hydrochloride **18b** (61 mg, 0.4 mmol, Aldrich, CAS No. 1115-59-9), and then Et<sub>3</sub>N (70  $\mu$ L, 0.5 mmol) was added. The resultant mixture was stirred for about 15 min, and then additional Et<sub>3</sub>N (70  $\mu$ L, 0.5 mmol) was added to give a solution pH of 9–10. The mixture was stirred for about 2 h and then diluted with ethyl acetate, washed with saturated aqueous NaHCO<sub>3</sub> solution, followed by saturated aqueous NaCl solution. The organic layer was dried over anhydrous sodium sulfate and concentrated under reduced pressure. The residue was purified by reverse phase preparative HPLC to afford compound **4o** (5.5 mg, 16%). <sup>1</sup>H NMR (400 MHz, methanol-*d*<sub>4</sub>):  $\delta$  8.13 (s, 1H), 7.41 (d,  $J = 4.8$  Hz, 1H), 7.18 (d,  $J = 4.8$  Hz, 1H), 4.78 (d,  $J = 5.6$  Hz, 1H), 4.36 (m, 1H), 4.25–4.08 (m, 7H), 3.83 (m, 2H), 1.33–1.23 (m, 12H). <sup>31</sup>P NMR (162 MHz, methanol-*d*<sub>4</sub>):  $\delta$  13.8. MS  $m/z = 570.0$  [ $M + 1$ ].

**(2*S*,2'*S*)-Bis(2-ethylbutyl) 2,2'-(((2*R*,3*S*,4*R*,5*R*)-5-(4-Aminopyrrolo[1,2-*f*]-[1,2,4]triazin-7-yl)-5-cyano-3,4-dihydroxytetrahydrofuran-2-yl)methoxy)phosphoryl)bis(azanediyl)dipropionate (4p).** To a suspension of compound **4** (52 mg, 0.18 mmol) and solid sodium bicarbonate (53 mg) in trimethyl phosphate (1.5 mL) at 0 °C was added POCl<sub>3</sub> (120 mg, 0.783 mmol). The mixture was stirred at 0 °C for 3 h, at which point a solution of **18a** (790 mg, 4.56 mmol) in MeCN (1 mL) was then added. The reaction mixture was stirred at 0 °C for 0.5 h, then triethylamine (0.1 mL) was added and stirred at rt for 0.5 h. The reaction mixture was diluted with ethyl acetate (10 mL), washed with water (10 mL), and concentrated under reduced pressure. The residue was purified by silica gel column chromatography (eluent, 50–100% ethyl acetate in hexanes gradient followed by 0–10% methanol in ethyl acetate gradient) to afford compound **4p** (71 mg, 58%). <sup>1</sup>H NMR (400 MHz, methanol-*d*<sub>4</sub>):  $\delta$  7.88 (s, 1H), 6.95 (d,  $J = 4.8$  Hz, 1H), 6.89 (d,  $J = 4.4$  Hz, 1H), 4.85 (d,  $J = 5.6$  Hz, 1H), 4.35–4.32 (m, 1H), 4.26–4.12 (m, 3H), 4.09–4.04 (m, 2H), 3.98–3.94 (m, 2H), 3.89–3.79 (m, 2H), 1.54–1.44 (m, 2H), 1.39–1.27 (m, 14H), 0.89 (t,  $J = 7.2$  Hz, 12H). <sup>31</sup>P NMR (162 MHz, methanol-*d*<sub>4</sub>):  $\delta$  13.83. MS  $m/z = 682.1$  [ $M + 1$ ].

## ■ ASSOCIATED CONTENT

### § Supporting Information

The Supporting Information is available free of charge on the ACS Publications website at DOI: 10.1021/acs.jmedchem.6b01594.

Homology model of HIV (1RTD<sup>32b</sup>) X-ray structure used to generate the EBOV model for **4tp** (PDB)

Homology model of HCV (4WTG<sup>32c</sup>) X-ray structure used to generate the EBOV model for **13tp** (PDB)

Molecular formula strings (CSV)

Assay methods, molecular modeling with RSV, Marburg and Sudan viruses, compound synthesis, and single crystal X-ray structure information (PDF)

### Accession Codes

The Cambridge Crystallographic Data Center (CCDC) numbers for the X-ray structures of compound **22b** and **4b** are 1445315 and 1525480, respectively.

## ■ AUTHOR INFORMATION

### Corresponding Author

\*E-mail: richard.mackman@gilead.com. Tel.: 650 522 5258.

### ORCID

Richard L. Mackman: 0000-0001-8861-7205

### Notes

Opinions, interpretations, conclusions, and recommendations are those of the authors and are not necessarily endorsed by the U.S. Army, U.S. Department of Health and Human Services, the Public Health Service, the Centers for Disease Control and Prevention, or the authors' affiliated institutions. Research was conducted under an IACUC approved protocol in compliance with the Animal Welfare Act, PHS Policy, and other Federal statutes and regulations relating to animals and experiments involving animals. The facility where this research was conducted is accredited by the Association for Assessment and Accreditation of Laboratory Animal Care, International and adheres to principles stated in the Guide for the Care and Use of Laboratory Animals, National Research Council, 2011. The authors declare no competing financial interest.

## ■ ACKNOWLEDGMENTS

We acknowledge the contributions of the following individuals at USAMRIID for participation: in vivo studies, J. Wells, K. Stuthman, N. Lackemeyer, S. Van Tongeren, G. Donnelly, J. Steffens, A. Shurtleff, L. Gomba, and J. Benko; scientific input, L. Welch, T. Bocan, A. Duplantier, R. Panchal, C. Kane, and D. Mayers (currently of Cocrystal Pharma, Inc.); and services performed, S. Tritsch, C. Retterer, D. Gharaibeh, T. Kenny, B. Eaton, G. Gomba, J. Nuss, and C. Rice. From Gilead Sciences we acknowledge K. Wang, K. Brendza, T. Alfredson, and L. Serafini who assisted with analytical methods, S. Bondy and R. Seemayer procured key raw materials, and L. Heumann, R. Polniaszcek, E. Rueden, A. ChtChemelinine, K. Brak, and B. Hoang contributed to synthesis, Yelena Zhrebina to chiral separations, and D. Babusis for DMPK sample analysis data. We also thank Curtis E. Moore from the Rheingold Laboratory, UC San Diego, for assistance in the solving of crystal structures. These studies were in part supported by The Joint Science and Technology Office for Chemical and Biological Defense (JSTO-CBD) of the Defense Threat Reduction Agency (DTRA) under Plan No. CB10218. CDC core funding supported the work done by M.K.L. at CDC.

## ■ ABBREVIATIONS USED:

BSL-4, biosafety level 4; EBOV, Ebola virus; EVD, Ebola virus disease; HEp-2, human epithelial type 2 cell; HMVEC-TERT, human foreskin microvascular endothelial cells; Huh-7, hepatocellular carcinoma cell; IACUC, Institutional Animal Care and Use Committee; IND, investigational new drug; LG, leaving group; log *D*, logarithm of distribution coefficient; Macro, human macrophage cells; MERS, Middle East respiratory syndrome; MT4, human leukemia T-cell; NHP, non-human primate; NMI, *N*-methylimidazole; NTP, nucleoside triphosphate; PBMC, peripheral blood mononuclear cell; PFP, pentafluorophenol; PNP, *p*-nitrophenol; Pol, polymerase; POLRMT, mitochondrial RNA polymerase; RSV, respiratory syncytial virus; SARS, severe acute respiratory syndrome; SD, standard deviation; SNI, single nucleotide incorporation; USAMRIID, United States Army Medical Research Institute of Infectious Diseases

## ■ REFERENCES

- (1) World Health Organization. *Ebola Situation Report—10 June 2016*. [http://apps.who.int/iris/bitstream/10665/208883/1/ebolasitrep\\_10Jun2016\\_eng.pdf?ua=1](http://apps.who.int/iris/bitstream/10665/208883/1/ebolasitrep_10Jun2016_eng.pdf?ua=1) (accessed Jul. 22, 2016).
- (2) World Health Organization. *Ebola Data and Statistics—11 May 2016*. <http://apps.who.int/gho/data/view Ebola-sitrep Ebola-summary-20160511?lang=en> (accessed Jul. 22, 2016).
- (3) Vetter, P.; Fischer, W. A. II; Schibler, M.; Jacobs, M.; Bausch, D. G.; Kaiser, L. Ebola Virus Shedding and Transmission: Review of Current Evidence. *J. Infect. Dis.* **2016**, *214*, S177–S184.
- (4) Mate, S. E.; Kugelman, J. R.; Nyenswah, T. G.; Ladner, J. T.; Wiley, M. R.; Cordier-Lassalle, T.; Christie, A.; Schroth, G. P.; Gross, S. M.; Davies-Wayne, G. J.; Shinde, S. A.; Murugan, R.; Sieh, S. B.; Badio, M.; Fakoli, L.; Taweh, F.; de Wit, E.; van Doremalen, N.; Munster, V. J.; Pettitt, J.; Prieto, K.; Humrighouse, B. W.; Ströher, U.; DiClaro, J. W.; Hensley, L. E.; Schoepp, R. J.; Safronetz, D.; Fair, J.; Kuhn, J. H.; Blackley, D. J.; Laney, A. S.; Williams, D. E.; Lo, T.; Gasasira, A.; Nichol, S. T.; Formenty, P.; Kateh, F. N.; De Cock, K. M.; Bolay, F.; Sanchez-Lockhart, M.; Palacios, G. Molecular Evidence of Sexual Transmission of Ebola Virus. *N. Engl. J. Med.* **2015**, *373*, 2448–2454.
- (5) Kuhn, J. H. *Filoviruses: A Compendium of 40 Years of Epidemiological, Clinical, and Laboratory Studies*; Calisher, C. H., Ed.; Springer: Wien, Austria, 2008.
- (6) Rougeron, V.; Feldmann, H.; Grard, G.; Becker, S.; Leroy, E. M. Ebola and Marburg Haemorrhagic Fever. *J. Clin. Virol.* **2015**, *64*, 111–119.
- (7) Qiu, X.; Wong, G.; Audet, J.; Bello, A.; Fernando, L.; Alimonti, J. B.; Fausther-Bovendo, H.; Wei, H.; Aviles, J.; Hiatt, E.; Johnson, A.; Morton, J.; Swope, K.; Bohorov, O.; Bohorova, N.; Goodman, C.; Kim, D.; Pauly, M. H.; Velasco, J.; Pettitt, J.; Olinger, G. G.; Whaley, K.; Xu, B.; Strong, J. E.; Zeitlin, L.; Kobinger, G. P. Reversion of Advanced Ebola Virus Disease in Nonhuman Primates with ZMapp. *Nature* **2014**, *514*, 47–53.
- (8) Thi, E. P.; Mire, C. E.; Lee, A. C. H.; Geisbert, J. B.; Zhou, J. Z.; Agans, K. N.; Snead, N. M.; Deer, D. J.; Barnard, T. R.; Fenton, K. A.; MacLachlan, I.; Geisbert, T. W. Lipid Nanoparticles siRNA Treatment of Ebola-Virus-Makona-Infected Nonhuman Primates. *Nature* **2015**, *521*, 362–365.
- (9) Tekmira Pharmaceuticals Corp. *Tekmira Provides Update on TKM-Ebola-Guinea*. <http://www.sec.gov/Archives/edgar/data/1447028/000117184315003522/newsrelease.htm>, 2015 (accessed Jul. 22, 2016).
- (10) Iversen, P. L.; Warren, T. K.; Wells, J. B.; Garza, N. L.; Mourich, D. V.; Welch, L. S.; Panchal, R. G.; Bavari, S. Discovery and Early Development of AVI-7537 and AVI-7288 For the Treatment of Ebola Virus and Marburg Virus Infections. *Viruses* **2012**, *4*, 2806–2830.
- (11) Oestereich, L.; Lüdtke, A.; Wurr, S.; Rieger, T.; Muñoz-Fontela, C.; Günther, S. Successful Treatment of Advanced Ebola Virus Infection With T-705 (favipiravir) in a Small Animal Model. *Antiviral Res.* **2014**, *105*, 17–21.
- (12) Smither, S. J.; Eastaugh, L. S.; Steward, J. A.; Nelson, M.; Lenk, R. P.; Lever, M. S. Post-exposure Efficacy of Oral T-705 (Favipiravir) Against Inhalational Ebola Virus Infection in a Mouse Model. *Antiviral Res.* **2014**, *104*, 153–155.
- (13) Sissoko, D.; Folkesson, E.; Abdoul, M.; Beavogui, A. H.; Gunther, S.; Shepherd, S.; Danel, C.; Mentre, F.; Anglaret, X.; Malvy, D. Favipiravir in Patients With Ebola Virus Disease: Early Results of the JIKI Trial in Guinea. *Conference on Retroviruses and Opportunistic Infections*, Seattle, WA, USA, Feb. 23–26, 2015, Abstract 103-ALB; CROI Foundation/IAS-USA: San Francisco, CA, USA, 2015.
- (14) McMullan, L. K.; Flint, M.; Dyall, J.; Albariño, C.; Olinger, G. G.; Foster, S.; Sethna, P.; Hensley, L. E.; Nichol, S. T.; Lanier, E. R.; Spiropoulou, C. F. The Lipid Moiety of Brincidofovir is Required For In Vitro Antiviral Activity Against Ebola Virus. *Antiviral Res.* **2016**, *125*, 71–78.
- (15) Warren, T. K.; Wells, J.; Panchal, R. G.; Stuthman, K. S.; Garza, N. L.; Van Tongeren, S. A.; Dong, L.; Retterer, C. J.; Eaton, B. P.; Pegoraro, G.; Honnold, S.; Bantia, S.; Kotian, P.; Chen, X.; Taubenheim, B. R.; Welch, L. S.; Minning, D. M.; Babu, Y. S.; Sheridan, W. P.; Bavari, S. Protection Against Filovirus Disease by a Novel Broad-Spectrum Nucleoside Analogue BCX4430. *Nature* **2014**, *508*, 402–405.
- (16) Henao-Restrepo, A. M.; Longini, I. M.; Egger, M.; Dean, N. E.; Edmunds, W. J.; Camacho, A.; Carroll, M. W.; Doumbia, M.; Draguez, B.; Duraffour, S.; Enwere, G.; Grais, R.; Gunther, S.; Hossmann, S.; Kondé, M. K.; Kone, S.; Kuisma, A.; Levine, M. M.; Mandal, S.; Norheim, G.; Riveros, X.; Soumah, A.; Trelle, S.; Vicari, A. S.; Watson, C. H.; Kéita, S.; Kieny, M. P.; Rottingen, J.-A. Efficacy and Effectiveness of an rVSV-Vectored Vaccine Expressing Ebola, Surface Glycoprotein: Interim Results From the Guinea Ring Vaccination Cluster-Randomised Trial. *Lancet* **2015**, *386*, 857–866.
- (17) Warren, T. K.; Jordan, R.; Lo, M. K.; Ray, A. S.; Mackman, R. L.; Soloveva, V.; Siegel, D.; Perron, M.; Bannister, R.; Hui, H. C.; Larson, N.; Strickley, R.; Wells, J.; Stuthman, K. S.; Van Tongeren, S. A.; Garza, N. L.; Donnelly, G.; Shurtleff, A. C.; Retterer, C. J.; Gharaibeh, D.; Zamani, R.; Kenny, T.; Eaton, B. P.; Grimes, E.; Welch, L. S.; Gomba, L.; Wilhelmsen, C. L.; Nichols, D. K.; Nuss, J. E.; Nagle, E. R.; Kugelman, J. R.; Palacios, G.; Doerffler, E.; Neville, S.; Carra, E.; Clarke, M. O.; Zhang, L.; Lew, W.; Ross, B.; Wang, Q.; Chun, K.; Wolfe, L.; Babusis, D.; Park, Y.; Stray, K. M.; Trancheva, I.; Feng, J. Y.; Barauskas, O.; Xu, Y.; Wong, P.; Braun, M. R.; Flint, M.; McMullan, L. K.; Chen, S. S.; Fearn, R.; Swaminathan, S.; Mayers, D. L.; Spiropoulou, C. F.; Lee, W. A.; Nichol, S. T.; Cihlar, T.; Bavari, S. Therapeutic Efficacy of The Small Molecule GS-5734 Against Ebola Virus in Rhesus Monkeys. *Nature* **2016**, *531*, 381–385.
- (18) Mehellou, Y.; Balzarini, J.; McGuigan, C. Aryloxy Phosphoramidate Triesters: A Technology For Delivering Monophosphorylated Nucleosides and Sugars Into Cells. *ChemMedChem* **2009**, *4*, 1779–1791.
- (19) Sofia, M. J.; Bao, D.; Chang, W.; Du, J.; Nagarathnam, D.; Rachakonda, S.; Reddy, P. G.; Ross, B. S.; Wang, P.; Zhang, H.-R.; Bansal, S.; Espiritu, C.; Keilman, M.; Lam, A. M.; Steuer, H. M. M.; Niu, C.; Otto, M. J.; Furman, P. A. Discovery of a  $\beta$ -D-2'-Deoxy-2'- $\alpha$ -Fluoro-2'- $\beta$ -C-Methyluridine Nucleotide Prodrug (PSI-7977) for the Treatment of Hepatitis C Virus. *J. Med. Chem.* **2010**, *53*, 7202–7218.
- (20) Lee, A. W.; He, G.-X.; Eisenberg, E.; Cihlar, T.; Swaminathan, S.; Mulato, A.; Cundy, K. C. Selective Intracellular Activation of a Novel Prodrug of the Human Immunodeficiency Virus Reverse Transcriptase Inhibitor Tenofovir Leads to Preferential Distribution and Accumulation in Lymphatic Tissue. *Antimicrob. Agents Chemother.* **2005**, *49*, 1898–1906.
- (21) Murakami, E.; Niu, C.; Bao, H.; Steuer, H. M. M.; Whitaker, T.; Nachman, T.; Sofia, M. A.; Wang, P.; Otto, M. J.; Furman, P. A. The Mechanism of Action of  $\beta$ -D-2'-Deoxy-2'-Fluoro-2'-C-Methylcytidine Involves a Second Metabolic Pathway Leading to  $\beta$ -D-2'-Deoxy-2'-Fluoro-2'-C-Methyluridine 5'-Triphosphate, A Potent Inhibitor of the

Hepatitis C Virus RNA-Dependent RNA Polymerase. *Antimicrob. Agents Chemother.* **2008**, *52*, 458–464.

(22) Cho, A.; Saunders, O. L.; Butler, T.; Zhang, L.; Xu, J.; Vela, J. E.; Feng, J. Y.; Ray, A. S.; Kim, C. U. Synthesis and Antiviral Activity of a Series of 1'-Substituted 4-Aza-7,9-Dideazaadenosine C-Nucleosides. *Bioorg. Med. Chem. Lett.* **2012**, *22*, 2705–2707.

(23) Mackman, R. L.; Parrish, J. P.; Ray, A. S.; Theodore, D. A. Methods and Compounds for Treating Paramyxoviridae Virus Infections. U.S. Patent 2011045102 July, 22, 2011.

(24) Patil, S. A.; Otter, P. B.; Klein, R. S. 4-Aza-7,9-Dideazaadenosine, A New Cytotoxic Synthetic C-Nucleoside Analogue of Adenosine. *Tetrahedron Lett.* **1994**, *35*, 5339–5342.

(25) Lou, Z.; Chen, G.; Xie, Y. Cyanoribofuranoside Compound and a Preparation Method Thereof. Chinese Patent CN 1137132 C Feb., 4, 2004.

(26) Yoshimura, Y.; Kano, F.; Miyazaki, S.; Ashida, N.; Sakata, S.; Haraguchi, K.; Itoh, Y.; Tanaka, H.; Miyasaka, T. Synthesis and Biological Evaluation of 1'-C-Cyano-Pyrimidine Nucleosides. *Nucleosides, Nucleotides Nucleic Acids* **1996**, *15*, 305–324.

(27) Kirschberg, T. A.; Mish, M.; Squires, N. H.; Zonte, S.; Aktoudianakis, E.; Metobo, S.; Butler, T.; Ju, X.; Cho, A.; Ray, A. S.; Kim, C. U. Synthesis of 1'-C-Cyano Pyrimidine Nucleosides and Characterization as HCV Polymerase Inhibitors. *Nucleosides, Nucleotides Nucleic Acids* **2015**, *34*, 763–785.

(28) Cho, A.; Zhang, L.; Xu, J.; Lee, R.; Butler, T.; Metobo, S.; Aktoudianakis, V.; Lew, W.; Ye, H.; Clarke, M.; Doerffler, E.; Byun, D.; Wang, T.; Babusis, D.; Carey, A. C.; German, P.; Sauer, D.; Zhong, W.; Rossi, S.; Fenaux, M.; McHutchison, J. G.; Perry, J.; Feng, J.; Ray, A. S.; Kim, C. U. Discovery of the First C-nucleoside HCV Polymerase Inhibitor (GS-6620) with Demonstrated Antiviral Response in HCV Infected Patients. *J. Med. Chem.* **2014**, *57*, 1812–1825.

(29) (a) Smith, J. T.; Elkin, J. T.; Reichert, W. M. Directed Cell Migration on Fibronectin Gradients: Effect of Gradient Slope. *Exp. Cell Res.* **2006**, *312*, 2424–2432. (b) Zhao, L.; Kroenke, C. D.; Song, J.; Piwnicka-Worms, D.; Ackerman, J. J. H.; Neil, J. J. Intracellular Water Specific MR of Microbead-Adherent Cells: The HeLa Cell Intracellular Water Exchange Lifetime. *NMR Biomed.* **2008**, *21*, 159–164.

(30) Clarke, M. O.; Mackman, R.; Byun, D.; Hui, H.; Barauskas, O.; Birkus, G.; Chun, B.-K.; Doerffler, E.; Feng, J.; Karki, K.; Lee, G.; Perron, M.; Siegel, D.; Swaminathan, S.; Lee, W. Discovery of  $\beta$ -D-2'- $\alpha$ -Fluoro-4'- $\alpha$ -Cyano-5-Aza-7,9-Dideaza Adenosine as a Potent Nucleoside Inhibitor of Respiratory Syncytial Virus With Excellent Selectivity Over Mitochondrial RNA and DNA Polymerases. *Bioorg. Med. Chem. Lett.* **2015**, *25*, 2484–2487.

(31) Feng, J.; Xu, Y.; Barauskas, O.; Perry, J. K.; Ahmadyar, S.; Stepan, G.; Yu, H.; Babusis, D.; Park, Y.; McCutcheon, K.; Perron, M.; Schultz, B. E.; Sakowicz, R.; Ray, A. S. Role of Mitochondrial RNA Polymerase in the Toxicity of Nucleotide Inhibitors of Hepatitis C Virus. *Antimicrob. Agents Chemother.* **2016**, *60*, 806–817.

(32) (a) Müller, R.; Poch, O.; Delarue, M.; Bishop, D. H. L.; Bouloy, M. Rift Valley Fever Virus L Segment: Correction of the Sequence and Possible Functional Role of Newly Identified Regions Conserved in RNA-Dependent Polymerases. *J. Gen. Virol.* **1994**, *75*, 1345–1352. (b) Huang, H.; Chopra, R.; Verdine, G. L.; Harrison, S. C. Structure of a Covalently Trapped Catalytic Complex of HIV-1 Reverse Transcriptase: Implications for Drug Resistance. *Science* **1998**, *282*, 1669–1675. (c) Appleby, T. C.; Perry, J. K.; Murakami, E.; Barauskas, O.; Feng, J.; Cho, A.; Fox, D.; Wetmore, D. R.; McGrath, M. E.; Ray, A. S.; Sofia, M. J.; Swaminathan, S.; Edwards, T. E. Structural Basis For RNA Replication by the Hepatitis C Virus Polymerase. *Science* **2015**, *347*, 771–775.

(33) For active site models of other filovirus polymerases see the [Supporting Information](#).

(34) Feng, J. Y.; Cheng, G.; Perry, J.; Barauskas, O.; Xu, Y.; Fenaux, M.; Eng, S.; Tirunagari, N.; Peng, B.; Yu, M.; Tian, Y.; Lee, Y.-J.; Stepan, G.; Lagpacan, L. L.; Jin, D.; Hung, M.; Ku, K. S.; Han, B.; Kitrinis, K.; Perron, M.; Birkus, G.; Wong, K. A.; Zhong, W.; Kim, C. U.; Carey, A.; Cho, A.; Ray, A. S. Inhibition of Hepatitis C Virus

Replication by GS-6620, a Potent C-Nucleoside Monophosphate Prodrug. *Antimicrob. Agents Chemother.* **2014**, *58*, 1930–1942.

(35) Butler, T.; Cho, A.; Kim, C. U.; Saunders, O. L.; Zhang, L. 1'-Substituted Carba-Nucleoside Analogs for Antiviral Treatment. U.S. Patent 2009041447 Apr., 22, 2009.

(36) Butler, T.; Cho, A.; Graetz, B. R.; Kim, C. U.; Metobo, S. E.; Saunders, O. L.; Waltman, A. W.; Xu, J.; Zhang, L. Processes and Intermediates for the Preparation of 1'-Substituted Carba-Nucleoside Analogs. U.S. Patent 20100459508 Sep., 20, 2010.

(37) Metobo, S. E.; Xu, J.; Saunders, O. L.; Butler, T.; Aktoudianakis, E.; Cho, A.; Kim, C. U. Practical Synthesis of 1'-Substituted Tubercidin C-Nucleoside Analogs. *Tetrahedron Lett.* **2012**, *53*, 484–486.

(38) Axt, S. D.; Badalov, P. R.; Brak, K.; Campagna, S.; Chtchemelinine, A.; Chun, B. K.; Clarke, M. O. H.; Doerffler, E.; Frick, M. M.; Gao, D.; Heumann, L. V.; Hoang, B.; Hui, H. C.; Jordan, R.; Lew, W.; Mackman, R. L.; Milburn, R. R.; Neville, S. T.; Parrish, J. P.; Ray, A. S.; Ross, B.; Rueden, E.; Scott, R. W.; Siegel, D.; Stevens, A. C.; Tadeus, C.; Vieira, T.; Waltman, A. W.; Wang, X.; Whitcomb, M. C.; Wolfe, L.; Yu, C.-Y. Methods For Treating Filoviridae Virus Infections. U.S. Patent 2015017934, Oct. 29, 2015.

(39) Krasovskiy, A.; Knochel, P. A LiCl-Mediated Br/Mg Exchange Reaction For the Preparation of Functionalized Aryl- and Heteroaryl-magnesium Compounds From Organic Bromides. *Angew. Chem., Int. Ed.* **2004**, *43*, 3333–3336.

(40) For a separate account describing the crystallization induced resolution of *p*-nitrophenolate 2-ethylbutyl-L-alaninate phosphoramidate see: Klasson, B.; Eneroth, A.; Nilson, M.; Pinho, P.; Samuelsson, B.; Sund, C. HCV Polymerase Inhibitors. European Patent IB2012056994 Dec. 5, 2012. The conditions in this patent were identified independently/concurrently with this report.

(41) Bahar, F. G.; Ohura, K.; Ogihara, T.; Imai, T. Species Difference of Esterase Expression and Hydrolase Activity in Plasma. *J. Pharm. Sci.* **2012**, *101*, 3979–3988.

(42) Jacobs, M.; Rodger, A.; Bell, D. D.; Bhagani, S.; Cropley, I.; Filipe, A.; Gifford, R. J.; Hopkins, S.; Hughes, J.; Jabeen, F.; Johannessen, I.; Karageorgopoulos, D.; Lackenby, A.; Lester, R.; Liu, R. S. N.; MacConnachie, A.; Mahungu, T.; Martin, D.; Marshall, N.; Mephram, S.; Orton, R.; Palmarini, M.; Patel, M.; Perry, C.; Peters, S. E.; Porter, D.; Ritchie, D.; Ritchie, N. D.; Seaton, R. A.; Sreenu, V. B.; Templeton, K.; Warren, S.; Wilkie, G. S.; Zambon, M.; Gopal, R.; Thomson, E. C. Late Ebola Virus Relapse Causing Meningoencephalitis: A Case Report. *Lancet* **2016**, *388*, 498–503.

(43) Schnirring, L. Youngest Ebola Survivor Leaves Guinea Hospital; Center For Infectious Disease Research and Policy, Minneapolis, MN, USA, Nov. 30, 2015; <http://www.cidrap.umn.edu/news-perspective/2015/11/youngest-ebola-survivor-leaves-guinea-hospital> (accessed Jul. 22, 2016).

(44) National Institutes of Health. PREVAIL Treatment Trial For Men With Persistent Ebola Viral RNA in Semen Opens in Liberia, Jul. 5, 2016; <https://www.nih.gov/news-events/news-releases/prevail-treatment-trial-men-persistent-ebola-viral-rna-semen-opens-liberia> (accessed, Jul. 22, 2016).